bioRxiv preprint doi: https://doi.org/10.1101/2024.05.20.594925; this version posted May 20, 2024. The copyright holder for this preprint (which was not certified by peer review) is the author/funder, who has granted bioRxiv a license to display the preprint in perpetuity. It is made available under aCC-BY-NC-ND 4.0 International license.

Title

Microscale sampling of the coral gastric cavity reveals a gut-like microbial community

Authors

Elena Bollati[1]*, David J. Hughes[2]*, David J. Suggett[3,4], Jean-Baptiste Raina[4] and Michael Kühl[1]

* these authors contributed equally to this work

[1] Marine Biology Section, Department of Biology, University of Copenhagen, 3000 Helsingør, Denmark

[2] National Sea Simulator, Australian Institute of Marine Science, Townsville, Queensland, 4810, Australia

[3] KAUST Reefscape Restoration Initiative (KRRI), King Abdullah University of Science and Technology, Thuwal, 23955, Saudi Arabia

[4] University of Technology Sydney, Climate Change Cluster, Faculty of Science, University of Technology Sydney, Ultimo, NSW, 2007, Australia

Correspondence to: Elena Bollati, elena.bollati@bio.ku.dk

ORCID

EB: 0000-0003-3536-4587

DJH: 0000-0003-3778-7460

DJS: 0000-0001-5326-2520

JBR: 0000-0002-7508-0004

MK: 0000-0002-1792-4790

The authors declare no competing interests.

bioRxiv preprint doi: https://doi.org/10.1101/2024.05.20.594925; this version posted May 20, 2024. The copyright holder for this preprint (which was not certified by peer review) is the author/funder, who has granted bioRxiv a license to display the preprint in perpetuity. It is made available under aCC-BY-NC-ND 4.0 International license.

Abstract

Animal guts contain numerous microbes, which are critical for nutrient assimilation and pathogen defence. While corals and other Cnidaria lack a true differentiated gut, they possess gastrovascular cavities (GVCs), semi-enclosed compartments where vital processes such as digestion, reproduction and symbiotic exchanges take place. The microbiome harboured in GVCs is therefore likely key to holobiont fitness, but remains severely understudied due to challenges of working in these small compartments. Here, we developed minimally invasive methodologies to sample the GVC of coral polyps and characterise the microbial communities harboured within. We used glass capillaries, low dead volume microneedles, or nylon microswabs to sample the gastric microbiome of individual polyps from six species of corals, then applied low-input DNA extraction to characterise the microbial communities from these microliter volume samples. Microsensor measurements of GVCs revealed anoxic or hypoxic micro-niches, which persist even under prolonged illumination with saturating irradiance. These niches harboured microbial communities enriched in putatively microaerophilic or facultatively anaerobic taxa, such as Epsilonproteobacteria. Some core taxa found in the GVC of *Lobophyllia hemprichii* from the Great Barrier Reef were also detected in conspecific colonies held in aquaria, indicating that these associations are unlikely to be transient. Our findings suggest that the coral GVC is chemically and microbiologically similar to the gut of higher Metazoa. Given the importance of gut microbiomes in mediating animal health, harnessing the coral "gut microbiome" may foster novel active interventions aimed at increasing the resilience of coral reefs to the climate crisis.

bioRxiv preprint doi: https://doi.org/10.1101/2024.05.20.594925; this version posted May 20, 2024. The copyright holder for this preprint (which was not certified by peer review) is the author/funder, who has granted bioRxiv a license to display the preprint in perpetuity. It is made available under aCC-BY-NC-ND 4.0 International license.

Introduction

The gastrointestinal tract of all animals, from invertebrates to humans, hosts countless microorganisms that play an integral part in the physiology and health of their host. For example, the human gut is estimated to contain over 100 trillion bacterial cells belonging to over 1000 taxa [1], which influence all aspects of human biology, from immunity to behaviour and mental health [2, 3]. Compared to mammals, invertebrate animals such as insects often harbour less diverse gut communities [4], which nonetheless have a profound impact on their host's fitness [5]. However, the field of gut microbiology is still in its infancy for non-model marine invertebrates. Such organisms are often very small and sometimes lack a true digestive tract, and their microbial communities are commonly characterised at the whole-organism level (i.e., bulk sampling strategy) without differentiating gastrointestinal communities from endosymbiotic or epibiotic communities [6, 7].

This bulk sampling strategy is also routinely employed for reef-building corals [8], which are sessile colonial organisms living in symbiosis with dinoflagellate microalgae (Symbiodiniaceae) that thrive from tropical to subtropical oceans. The algal symbionts provide up to 80% of the coral's metabolic requirements via translocation of photosynthetically-fixed carbon, while the rest of the coral energy budget is met through heterotrophic feeding [9]. Prey, such as zooplankton, is digested in the gastrovascular cavity (GVC), a semi-enclosed compartment that shares many commonalities with the digestive tracts of higher Metazoa despite lacking the degree of differentiation observed in true guts [7, 10, 11]. The coral GVC is lined by endodermal tissue, and is separated from the surrounding environment by the polyp's mouth and actinopharynx. Many central processes of holobiont physiology take place in the GVC: digestion, symbiont acquisition and expulsion, reproduction, and circulation of fluids and nutrients between inter-connected polyps [7]. Due to its morphology, the coral GVC likely presents micro-gradients not unlike those observed in bilaterian guts [7]. For example, while oxygen concentration in the external diffusive boundary layer (DBL) and in the upper GVC is primarily driven by diel light fluctuations [11, 12], a study performed on one coral species has reported a steep oxycline deeper in the GVC, leading to an anoxic zone at the bottom that can persist even under prolonged illumination [11]. Other studies have shown a pH decrease of up to one unit, as well as a decrease in the concentration of calcium ions [13, 14]. This limited microenvironmental evidence suggests that the coral GVC could be a hypoxic or even anoxic cavity, rich in carbohydrates and other metabolites from heterotrophic feeding. This would make it an ideal environment to harbour a specialised microbial community, which may play important roles in holobiont health similarly to the gut microbiome of higher metazoans.

bioRxiv preprint doi: https://doi.org/10.1101/2024.05.20.594925; this version posted May 20, 2024. The copyright holder for this preprint (which was not certified by peer review) is the author/funder, who has granted bioRxiv a license to display the preprint in perpetuity. It is made available under aCC-BY-NC-ND 4.0 International license.

Coral microbiomes have gained considerable attention in recent years due to their potential role in mitigating the adverse effects of ocean warming on reefs [15, 16], which causes recurrent coral bleaching events and poses the greatest threat to the survival of coral reefs [17]. To mitigate this, much research has been directed towards manipulative interventions that may increase the resilience of corals to bleaching events [18]. One of the more promising approaches involves the administration of probiotics, consortia of beneficial bacteria isolated from native coral microbiomes, which can reduce the negative effects of heat stress on the coral holobiont [19–23]. However, we still do not know how beneficial bacteria increase coral fitness [24], and more generally, what the functional role of most coral-associated bacteria is [25–28]. Microhabitat specificity is intimately linked with function [29], and communities hosted in different compartments within coral polyps (e.g., the GVC, mucus layer, tissue, skeleton) often have very different composition, functional profiles, and responsiveness to environmental change [30–34]. Bulk sampling strategies cannot identifying core bacteria that are exclusively associated with specific microhabitats (such as the algal symbiont cells) [35], an issue that hinders meaningful functional profiling. In this context, microscale sampling methods provide an invaluable tool to investigate individual microniches, including the GVC, and to unveil the role of their associated communities in holobiont health and resilience.

Technical challenges associated with sampling the coral GVC have resulted in very few attempts to characterise this specific microbiome. Using a glass microcapillary inserted through the mouth of anaesthetised polyps, Agostini et al. [11] sampled the gastric fluid from several *Galaxea fascicularis* polyps and identified a number of bacterial taxa by subcloning amplicons of 16S rDNA. Construction of a single library required pooling of approximately 0.5 mL of gastric fluid, sampled from ten polyps belonging to the same parental colony [11]. A second approach was proposed by Tang et al. [36], who collected gastric fluid from the same coral species (10-20 µL per polyp) by piercing the oral disc with a syringe and needle, subsequently plating the fluids on a rich medium (Marine Agar) and sequencing 16S rDNA from the bacterial colonies that formed. While these two approaches enabled characterisation of some GVC bacterial taxa to pioneer the study of coral GVC communities, both have limitations. Specifically, Tang et al. [36] only characterised the culturable fraction of the GVC microbiome, whilst Agostini et al. [11] avoided culturing by pooling multiple samples to obtain sufficient fluid volume. Pooling multiple samples across separate polyps not only affects the ability to analyse a large number of replicates or treatments, but also precludes the investigation of other coral species with even smaller GVCs or the characterisation of GVC heterogeneity within colonies.

bioRxiv preprint doi: https://doi.org/10.1101/2024.05.20.594925; this version posted May 20, 2024. The copyright holder for this preprint (which was not certified by peer review) is the author/funder, who has granted bioRxiv a license to display the preprint in perpetuity. It is made available under aCC-BY-NC-ND 4.0 International license.

Recently, a novel DNA extraction method was introduced to enable the recovery of metagenomic-quality microbial DNA from small volumes of seawater [37]. This novel method applies a physical or chemical lysis step followed by DNA recovery on paramagnetic beads to extract DNA from samples as small as 10 µL (physical lysis) or 1 µL (chemical lysis), yielding results comparable to those achieved from filtering 2 L of seawater and extracting DNA using a standard extraction kit [37]. In our present study, we therefore developed different microscale methods to sample the GVC in combination with this low-input DNA extraction protocol to characterise the microbial communities of the GVC of individual polyps for multiple coral taxa from the Great Barrier Reef (GBR). In parallel, we characterised the oxygen microenvironment experienced by these microbial communities *in hospite* using microsensors to investigate habitat specificity and potential functional profiles of the coral GVC microbiome.

Methods

Coral collection and aquarium maintenance

Great Barrier Reef (GBR) corals. Colonies of *Coelastrea aspera*, *Dipsastraea favus*, *Fungia fungites*, *Favites pentagona*, *Galaxea fascicularis* and *Lobophyllia hemprichii* (n = 4-6 per species, Supplementary Table S1, Supplementary Fig. 1) were collected from the reef flat of Heron Island (Great Barrier Reef, Australia) in April 2021.

Aquarium corals. Captive colonies of 6 genotypes of *L. hemprichii* originating from the Great Barrier Reef were obtained from the Australian ornamental trade in 2022 and maintained in aquaria at the University of Technology Sydney. Colonies were fragmented to obtain 11 sub-colonies, each with 1-3 polyps connected by tissue, yielding a total of 19 polyps (Supplementary Table S1, Supplementary Fig. 1).

Detailed information on coral sourcing and rearing conditions is provided in the Supplementary Materials (Sections 1-2).

Micro-sensing and -sampling setup

Microsensor measurements and sampling of GVC fluid were performed in a flow chamber (Fig. 1a,b) connected to an adjustable water pump placed in a 15 L reservoir containing seawater taken from the same environment as the corals; i.e., reef water via the Heron Island Research station supply system for GBR corals, or from the UTS holding tank for aquarium corals. Flow was adjusted to ~1 cm s^{-1}, and temperature was set to 25°C with a 25W

bioRxiv preprint doi: https://doi.org/10.1101/2024.05.20.594925; this version posted May 20, 2024. The copyright holder for this preprint (which was not certified by peer review) is the author/funder, who has granted bioRxiv a license to display the preprint in perpetuity. It is made available under aCC-BY-NC-ND 4.0 International license.

heater in the reservoir. Illumination was provided by an aquarium LED unit (Prime 16HD, Aqua Illuminations, Ames, IA, USA). A stereo microscope and/or a digital USB microscope (Dino-Lite Edge, AnMo Electronics Corporation, Taipei, Taiwan) enabled visualisation of the coral polyp mouth (Fig. 1b). Prior to performing microsensor profiles on each polyp, the bottom of the gastric cavity was identified by inserting a thin (~75-100 µm wide) glass capillary mounted in a micromanipulator (MM33; Märzhäuser GmbH, Germany) and recording the depth at which it flexed slightly.

Gastric cavity fluid sampling

Capillary method: GVC fluid extraction of GBR corals was performed with glass capillaries ~75-100 µm diameter, produced by pulling glass Pasteur pipettes on a flame. The capillary was mounted on a micromanipulator (Fig. 1a) and connected to a 50 mL syringe via silicone tubing. Prior to sampling, the capillary was sterilised with 10% bleach and 80 % ethanol, then rinsed with Milli-Q water. The capillary was preloaded with Milli-Q water, which was released to equalise the pressure inside the flow chamber once the desired sampling depth was reached. After equalisation, the capillary was moved to just above the polyp mouth using the micromanipulator, then lowered into the GVC to 50% of the polyp depth before slowly collecting ~20-50 µL of fluid over 45-60 s. The fluid was collected into a 1.8 mL cryovial (CryoPure, Sarstedt, Nürnberg, Germany) and homogenised by pipetting. A detailed sampling protocol including all sterilisation and equalisation procedures is provided in the Supplementary Materials (Section 3).

Immediately after homogenisation, a 5 µL subsample was fixed in 2% glutaraldehyde in 3× PBS (final volume 100 µL) for flow cytometry analysis, incubated for 20 minutes and then snap frozen in liquid nitrogen. The remaining fluid (typically 15-30 µL total volume depending on polyp size) was snap-frozen immediately for later DNA extraction. Three polyps per species were sampled with this method (except for *F. fungites*, a non-colonial coral, for which only a single polyp was sampled). The same sampling approach was used to collect water samples from the diffusive boundary layer (DBL) of each coral, about 30-50 µm above the oral disk surface and equidistant between the mouth and the polyp/corallite wall, and from the overlying seawater.

Needle method; Needle sampling of GVC fluid was performed on aquarium *L. hemprichii* polyps using a sterile low dead volume needle (34G, 9 mm long; The Invisible Needle, TSK, Vancouver, BC, Canada) connected to a 1 mL Luer lock syringe (Fig. 1c,d). Each coral was positioned so that the mouth opening was as close as possible

bioRxiv preprint doi: https://doi.org/10.1101/2024.05.20.594925; this version posted May 20, 2024. The copyright holder for this preprint (which was not certified by peer review) is the author/funder, who has granted bioRxiv a license to display the preprint in perpetuity. It is made available under aCC-BY-NC-ND 4.0 International license.

to the water surface, while keeping the entire animal submerged, in order to minimise the distance travelled by the needle outside the cavity. The syringe was mounted on the micromanipulator (Fig. 1c) and the needle lowered vertically into the polyp mouth using manual control. Once the needle tip disappeared fully inside the mouth (Fig. 1d), the syringe plunger was pulled very slowly in order to collect ~100 µL of gastric fluid. Fluid was collected into a sterile (UV radiation cross-linked for 1 hour) 1.5 mL centrifuge tube and immediately frozen at -80°C.

Swab method: Swab sampling of the GVC of each aquarium *L. hemprichii* polyp was performed immediately after needle sampling. A nylon swab of 0.8 mm diameter (TX730, Texwipe, Kernersville, NC, USA), which had been previously sterilised (UV radiation cross-linking for 1 hour), was mounted on the micromanipulator using a plastic pipette tip (P100) as an adapter. Using the micromanipulator manual controls, the swab was lowered into the flow chamber and into the polyp mouth, where it was then moved back and forth along the x and y axes for approximately five seconds to ensure good contact with the cavity surface (Fig. 1e). The swab was then withdrawn and removed from the micromanipulator. The tip was placed inside a cross-linked 1.5 mL centrifuge tube and cut with sterile scissors, before placing the tube in a -80°C freezer. Contamination of such sampling by seawater and mucus could be minimized by lowering the water level before sampling the GVC.

Oxygen microprofiling

Microsensor profiling was performed using a Clark-type O_2 microsensor (OX50, 50 µm tip diameter with a slender shaft; Unisense, Denmark) in both darkness, and under a saturating photon scalar irradiance (400-700 nm) of 650 µmol photons m^{-2} s^{-1}. Oxygen microsensors were calibrated at experimental temperature and salinity using air-saturated aquarium seawater (100%) and fully deoxygenated seawater (0% O_2, achieved using a Na_2SO_3 solution). Prior to measurement, the coral was exposed to saturating light or darkness for 20 min to allow O_2 concentration gradients to reach steady-state [38]. The microsensor tip was then manually positioned at the polyp's mouth using the micromanipulator. For measurements in darkness, 20 µmol photons m^{-2} s^{-1} of green light were administered briefly to help locate the polyp mouth. Depth profiles of O_2 concentration were measured down into the gastric cavity in vertical steps of 100 µm, with 3 s waiting time before each measurement, and a 1 s measuring period. The maximum depth limit for each profile was set to 80% of the total polyp depth measured in the respective light condition to minimise the chance of microsensor damage. Three vertical profiles were recorded consecutively for each polyp under each light condition. Three polyps per species were targeted for microprofiling (the same polyps used for gastric fluid sampling). Due to logistical issues, however, only a single polyp was successfully measured

bioRxiv preprint doi: https://doi.org/10.1101/2024.05.20.594925; this version posted May 20, 2024. The copyright holder for this preprint (which was not certified by peer review) is the author/funder, who has granted bioRxiv a license to display the preprint in perpetuity. It is made available under aCC-BY-NC-ND 4.0 International license.

for *F. fungites*, and no polyp was successfully measured for *F. pentagona* and *G. fascicularis*. For one polyp of *L. hemprichii*, a time series of oxygen concentration was also recorded in darkness while holding a microsensor at 4 mm depth (1.2 mm from the GVC bottom) for 75 minutes.

Bacterial cell counts

Counts of bacterial cells in the fixed gastric cavity fluid were conducted using flow cytometry (CytoFLEX LX, Beckman Coulter, USA), with filtered MilliQ water as the sheath fluid and a flow rate of 25 µL min^{-1}. Fixed gastric cavity fluid was stained with SYBR Green (final concentration 1:10,000) for 15 minutes in the dark. For each sample, forward scatter (FSC), side scatter (SSC), and green fluorescence (488 nm, SYBR) were recorded [39].

DNA extraction and 16S rDNA metabarcoding

DNA extraction from fluid samples (capillary GVC, DBL and seawater samples; needle GVC and seawater samples) was performed under a UV-clean hood using a low-input protocol (100 µL or 10 µL physical lysis extraction, Supplementary Table S1) described in Bramucci et al. [37]. All tubes and reagents (except ethanol and magnetic beads) were UV-sterilized for 1 h in a UV-crosslinker (CL-1000 Ultraviolet Crosslinker, UVP). Swab GVC and seawater samples were thawed and sonicated for 5 min at 4°C, before performing the same 100 µL physical lysis extraction protocol ensuring at each step that the buffer covered the swab tip. Swabs were removed from the tubes with a P1000 pipette before adding the magnetic beads. Extractions were performed in batches of 8 or 16 samples, and an extraction blank was included in each batch. Then, 5 µL of extracted DNA sample was used as PCR template and amplified using 16S V3-V4 primers with Illumina adapters (341F: **TCGTCGGCAGCGTCAGATGTGTATAAGAGACAG**CCTAYGGGRBGCASCAG and 805R: **GTCTCGTGGGCTCGGAGATGTGTATAAGAGACAG**GGACTACNNGGGTATCTAAT; adapters in bold) in a 30 µL reaction volume containing: 0.6 µL Velocity polymerase (Meridian Bioscience, Cincinnati, OH, USA), 6 µL Velocity buffer, 1.2 µL of each 10 µM primer, 3 µL of 10 µM dNTPs, 1 µL BSA (0.1 mg mL^{-1}, final concentration) and 12 µL PCR water. The amplification cycle was 98°C for 2 min, followed by 30 cycles of 98°C:30 sec, 55°C:30 sec and 72°C:30 sec, followed by a 10 min final elongation at 72°C. Amplicons were visualised on a gel before being submitted to the Australian Genome Resource Facility (Melbourne, VIC, Australia) for indexing, sequencing on Illumina MiSeq in two separate batches (run 1 = GBR corals; run 2 = UTS aquarium corals) and demultiplexing.

bioRxiv preprint doi: https://doi.org/10.1101/2024.05.20.594925; this version posted May 20, 2024. The copyright holder for this preprint (which was not certified by peer review) is the author/funder, who has granted bioRxiv a license to display the preprint in perpetuity. It is made available under aCC-BY-NC-ND 4.0 International license.

225

226 Sequencing data processing

227 All analysis was performed in R v4.1.1. Adaptors and primers were removed from demultiplexed reads using
228 *cutadapt* v4.4 [40], and the *dada2* pipeline (v1.22) was then applied separately to each sequencing run in order to
229 appropriately model the run-specific error rates [41]. Run 1 reads were truncated at 250 bp (forward) and 235 bp
230 (reverse), while run 2 reads were truncated at 270 bp (forward) and 250 bp (reverse). The maximum number of
231 expected errors was set to 2 for both runs.

232

233 As low-input DNA extraction methods are very sensitive to contamination, a stringent decontamination pipeline
234 was implemented as recommended by Bramucci et al. [37]. Two extraction negatives and four PCR negatives
235 were included in sequencing run 1, and three extraction negatives were included in sequencing run 2, along with
236 three sampling negative controls (cross-linked MilliQ water collected near the flow chamber either via needle or
237 swab at the end of all GVC sampling). For run 1, extraction contaminants were defined as ASVs that made up
238 more than 0.03% of processed reads in each extraction negative control. PCR contaminants were defined as ASVs
239 that were present in any amount in each of the PCR negative controls (with the exception of one PCR negative
240 control, which was mislabelled and discarded). For run 2, all ASVs found in the extraction negative controls were
241 classified as contaminants since the PCR negative control could not be sequenced. In addition, ASVs that made
242 up more than 0.03% of processed reads in the sampling negative controls were classified as contaminants. ASV
243 tables from run 1 and 2 were merged, and all contaminant sequences identified in either batch were removed from
244 all samples. After removal of contaminants and negative controls, taxonomy was assigned based on the Silva
245 database v138.1 [42] using the default *dada2* settings [41]. Sequences that were identified as mitochondria,
246 chloroplasts or eukaryotes were removed along with any samples that had zero remaining ASVs. Additional *L.*
247 *hemprichii* GVC samples ($n = 10$) which had been collected during methods optimisation were also removed from
248 the dataset at this point. Rarefaction curves (Supplementary Fig. S2) were produced and inspected using the *vegan*
249 v2.6-4 [43] package. As rarefaction curves indicated that sufficient sequencing depth had been achieved, no
250 rarefaction was applied to the dataset.

251

252 Statistical analysis

253 Shannon's H index was calculated to estimate alpha diversity of GBR corals using *phyloseq* v1.42 [44], while
254 beta diversity was assessed via nonmetric multidimensional scaling (NMDS) of Bray-Curtis dissimilarity in

bioRxiv preprint doi: https://doi.org/10.1101/2024.05.20.594925; this version posted May 20, 2024. The copyright holder for this preprint (which was not certified by peer review) is the author/funder, who has granted bioRxiv a license to display the preprint in perpetuity. It is made available under aCC-BY-NC-ND 4.0 International license.

vegan. For univariate data (alpha diversity, GVC depth, cell counts), homogeneity of variance was tested via Levene's test before applying parametric (t-test, paired t-test, ANOVA or RM-ANOVA) or non-parametric (Kruskal-Wallis) statistics. Post-hoc testing was carried out via Tukey test (following ANOVA) or Dunn's test (following Kruskal-Wallis) when all pairwise comparisons were of interest, or alternatively via adjusted pairwise t-tests when only a selection of comparisons was of interest. Groups that contained fewer than three data points (e.g. *F. fungites*) were removed before performing any statistical analysis. Count data were square-root transformed, and proportional data were arcsine square-root transformed before applying statistics. Wherever multiple tests were performed on the same dataset, P values were adjusted using the Benjamini-Hochberg correction. Alpha was set to 0.05.

To compare beta diversity between groups, singleton ASVs were removed from the dataset, then homogeneity of dispersion was tested using *betadisper* in *vegan*. PERMANOVA was used to test for significant difference between groups, wherever dispersion was deemed homogeneous, while ANOSIM was used in cases of non-homogeneous dispersion. All multivariate tests were permuted 1000 times. For GBR corals, differentially abundant taxa were identified by aggregating data to each taxonomic level and performing GLM tests on centred log ratio (clr)-transformed data in *ALDEx2* v1.26.0 [45].

Core microbiome analysis was performed in *microbiome* v1.16.0 [46]. Core taxa for each group were identified as taxa that made up more than 0.01% of the community in more than 50% of samples for that group.

Metagenomic predictions

Metagenomes were predicted from ASVs using PICRUSt2 v2.4.1 [47], and KO identifiers from the Kyoto Encyclopedia of Genes and Genomes (KEGG) were used to identify different predicted functions within each community [48]. This analysis was only performed on the *L. hemprichii* dataset due to the higher replication and lower dispersion in GVC community composition compared to the other GBR corals.

Seven metabolic marker genes (see Discussion for in-depth rationale) were identified from the literature [49, 50]. These were two high-affinity terminal oxidases, cytochrome c oxidase cbb3-type subunit I (*ccoN*, K00404), and cytochrome bd ubiquinol oxidase subunit I (*cydA*, K00425); two low-affinity terminal oxidases, cytochrome c oxidase aa3-type subunit I (*ctaD*, K02274), and cytochrome o ubiquinol oxidase subunit I (*cyo3*, K02298); the anaerobic transcription factor CRP/FNR family transcriptional regulator (*fnr*, K01420); the nitric oxide reductase

bioRxiv preprint doi: https://doi.org/10.1101/2024.05.20.594925; this version posted May 20, 2024. The copyright holder for this preprint (which was not certified by peer review) is the author/funder, who has granted bioRxiv a license to display the preprint in perpetuity. It is made available under aCC-BY-NC-ND 4.0 International license.

subunit B (*norB,* K04561); and the catalase gene (*CAT*, K03781). ASVs were classified based on the presence/absence of each functional gene in their predicted metagenome, and the cumulative abundance of ASVs containing each functional gene was calculated for each sample. Taxa containing either *ccoN* or *cydA* were grouped as "High affinity", and taxa containing either *ctaD* or *cyo3* were grouped as "Low affinity". We emphasise that these functional profiles were based exclusively on predicted metagenomes rather than metagenomic data, therefore they do not represent the true abundance of these metabolic genes.

Results

Great Barrier Reef corals: gastric cavity microenvironment

To characterise the GVC of GBR corals physically and chemically, we measured GVC depth and performed microsensor measurements of oxygen concentration under saturating light and in darkness. Median GVC depth measured in the dark ranged between 0.2 mm for *C. aspera* to 6.5 mm for *L. hemprichii*, with the latter significantly deeper than in most other species (Supplementary Fig. S3) (one-way ANOVA, $F_{3,8}$=7.46, P=0.011, followed by Tukey' HSD test, Supplementary Table S2). GVC depth remained unaltered in the light for *L. hemprichii*, *F. fungites*, and *C. aspera*, whereas cavities contracted by 0.5 mm and 1-1.4 mm for *D. favus* and *G. fascicularis*, respectively (Supplementary Fig. S3).

Microsensor measurements showed that for most coral species examined (with the exception of *F. fungites*), O_2 concentrations in the GVC were responsive to the light/dark cycle, with hyperoxic conditions generally detected under sustained illumination and anoxic conditions developing in the dark (Fig. 2). The GVCs of *D. favus*, *C. aspera* and *L. hemprichii* exhibited an oxycline in the light, with an anoxic region detected in the lower region even under saturating irradiance in some polyps (Fig. 2a,c,d,e). In darkness, the *D. favus* and *C. aspera* GVCs were predominantly anoxic (Fig. 2a,c,e), while *L. hemprichii* exhibited a normoxic/hypoxic region in the upper 1-2 mm of the GVC (Fig. 2e,f). *F. fungites* exhibited a unique GVC oxygen profile, with normoxic conditions maintained throughout the vast majority of the cavity regardless of illumination (Fig. 2b,f). Overall, potential permanently hypoxic or anoxic habitats were identified in the lower GVC of three out of four coral species investigated (Fig. 2e). Oxygen levels measured in the lower GVC were comparable with those reported from the lumen of mammalian hindguts, as well as different regions from invertebrate guts (Fig. 2f, Supplementary Table S3). Holding a microsensor in the hypoxic region close to the bottom of the GVC of *L. hemprichii* in darkness revealed that O_2 concentration was not constant over time (Supplementary Fig. S4). Small fluctuations between 0

bioRxiv preprint doi: https://doi.org/10.1101/2024.05.20.594925; this version posted May 20, 2024. The copyright holder for this preprint (which was not certified by peer review) is the author/funder, who has granted bioRxiv a license to display the preprint in perpetuity. It is made available under aCC-BY-NC-ND 4.0 International license.

and 5 µM were observed for the first 40 minutes of darkness, followed by much larger fluctuations between 0 and 100 µM over several hours (Supplementary Fig. S4).

Great Barrier Reef corals: GVC microbial community

We sampled the GVC fluid of GBR corals using the glass capillary method, and used the extracted fluid to perform bacterial cell counts and metabarcoding via 16S rDNA sequencing to characterise their gastric microbial community. Median bacterial cell counts in the GVC fluid ranged from 230,000 cells mL^{-1} (*L. hemprichii*) to 1,250,000 cells mL^{-1} (*C. aspera* and *F. fungites*), while median cell numbers in the DBL were similar across species (ranging between 420,000 in *G. fascicularis* and 614,000 cells mL^{-1} in *C. aspera*) (Fig. 3a). A significant interaction was observed between coral species and sample type (two-way ANOVA, $F_{6,24}$=2.87, P=0.030, Supplementary Table S4); however, subsequent post-hoc pairwise t-tests did not identify specific differences between groups after adjusting for multiple testing, likely due to the small sample size (Supplementary Table S4). Median alpha diversity in the GVC (Shannon's H index) ranged from 3.86 (*F. fungites*, single data point) to 6.81 (*C. aspera*); diversity was significantly different between groups (one-way ANOVA, $F_{9,28}$=5.03, P<0.001), and in particular it was lower in both the *G. fascicularis* GVC and DBL compared to seawater (adjusted P<0.05 in post-hoc pairwise t-tests) (Fig. 3b, Supplementary Table S5).

Beta diversity plots based on Bray-Curtis dissimilarity (Fig. 4a) showed that the seawater community remained similar throughout the 8-day sampling effort. Dispersion was significantly different between sampling locations (*betadisper*, 1000 permutations, F=20.04, P<0.001, Supplementary Table S5) but not between coral species (F=0.25, P=0.941) or replicate groups (F=2.27, P=0.068). Samples collected from the DBL clustered more closely together and closer to seawater, while samples collected from the GVC had greater dispersion with some replicates appearing distant not only from seawater or DBL samples, but also from other GVC samples (Fig. 4a). PERMANOVA on Bray-Curtis dissimilarity indicated that replicate groups were significantly different from each other (9999 permutations, F=2.09, R^2=0.48 p<0.001. Supplementary Table S6).

Differential abundance analysis performed on taxonomically aggregated data highlighted one significantly different taxon at the phylum level (Spirochaetota, adjusted P=0.006) between coral species and sampling locations (GVC, DBL, and seawater), four at the class level (including Epsilonproteobacteria, formerly Campylobacteria, adjusted P=0.035, and Anaerolineae, adjusted P=0.048), six at the order level (including

bioRxiv preprint doi: https://doi.org/10.1101/2024.05.20.594925; this version posted May 20, 2024. The copyright holder for this preprint (which was not certified by peer review) is the author/funder, who has granted bioRxiv a license to display the preprint in perpetuity. It is made available under aCC-BY-NC-ND 4.0 International license.

Campylobacterales, adjusted P=0.014), seven at the family level (including EC94, adjusted P=0.007), and 12 at the genus level (including *Thiovulum*, adjusted P=0.018) (Supplementary Table S7).

Differentially abundant taxa that appeared enriched in coral samples based on graphical examination are presented in Fig. 4b. Epsilonproteobacteria (formerly Campylobacteria) appeared enriched in coral GVCs, particularly in *L. hemprichii* (Fig. 4b). Anaerolineae were absent from seawater, from the *L. hemprichii* DBL and from the *G. fascicularis* GVC, but they were detected in the GVC and DBL of all other corals (Fig. 4b). The Gammaproteobacteria family EC94 was almost exclusively found in the *L. hemprichii* GVC (as well as in much smaller proportion in the *F. pentagona* GVC, Fig. 4b). The Epsilonproteobacteria genus *Thiovulum* was exclusively found in *L. hemprichii*, predominantly in the GVC as well as in very small proportion in a single sample from the DBL (Fig. 4b). Two taxa that have previously detected inside coral tissue as cell-associated microbial aggregates (CAMAs), *Endozoicomonas* and *Simkania* [51], had low abundance in the dataset. *Endozoicomonas* contributed to <1% of the community in all samples with the exception of the *F. pentagona* GVC (median = 1.8%) and DBL (median = 2.1%). *Simkania* were absent from seawater and all coral samples with the exception of a single sample of each of the following: *G. fascicularis* GVC (1.4%), *D. favus* GVC (0.76%), *F. fungites* DBL (0.84%) and *C. aspera* DBL (0.14%).

The *L. hemprichii* GVC microbiome in aquarium and GBR corals

Next, we investigated whether core patterns in GVC microbial community composition exist across different environments (i.e., on the reef and in captivity). We sampled three additional colonies of *L. hemprichii*, then resampled all six colonies after seven days in a flow-through system with natural GBR seawater. We then compared these with GVC samples collected from aquarium colonies of the same species, which had been obtained through a commercial provider and kept long-term in an artificial seawater system.

Alpha diversity of GBR and aquarium *L. hemprichii* was significantly different between sample types (i.e., seawater; GVC and DBL of aquarium *L. hemprichii*; GVC and DBL of GBR *L. hemprichii* on the day of collection; GVC and DBL of GBR *L. hemprichii* 7 days after collection; one-way ANOVA, $F_{5,56}=20$, $P<0.001$). However, post-hoc pairwise comparisons showed no significant differences between GVC communities in GBR *L. hemprichii* (whether on the day of collection or 7 days later) and in aquarium *L. hemprichii* (Fig. 5a), with the only significant differences being within samples collected from different locations (GVC vs DBL vs seawater, Supplementary Table S8). All environments tested (i.e., GVC, DBL and seawater) clearly clustered using NMDS

bioRxiv preprint doi: https://doi.org/10.1101/2024.05.20.594925; this version posted May 20, 2024. The copyright holder for this preprint (which was not certified by peer review) is the author/funder, who has granted bioRxiv a license to display the preprint in perpetuity. It is made available under aCC-BY-NC-ND 4.0 International license.

of Bray-Curtis dissimilarity. Clustering by sample type was significant (R^2 of 0.8; ANOSIM, 1000 permutations, P<0.001, Fig. 5b), and post-hoc pairwise comparisons confirmed that all groups were significantly different from each other (adjusted P<0.05, Supplementary Table S9). Seawater samples from the GBR formed a tight cluster, as did samples from the DBL of GBR *L. hemprichii* on the day of collection, while GVC fluid samples from both GBR and aquarium corals exhibited a wider spread (Fig. 5b). Interestingly, GVC and DBL samples from the same GBR *L. hemprichii* colonies appeared to diverge from each other 7 days after collection, and the same GVC samples clustered relatively close to those collected from aquarium *L. hemprichii* colonies (Fig. 5b). *Endozoicomonas* were absent from aquarium *L. hemprichii* samples, and *Simkania* were only detected in very low concentration (<0.1%) in two samples collected from adjacent mouths of a single individual.

Core microbiome analysis revealed that the DBL microbiome of *L. hemprichii* from the GBR was very variable in time (only 13.8% of the core ASVs present at the first time point were also identified as core ASVs from DBL samples at the second time point). In contrast, 64.3% of core ASVs detected in the GVC of GBR *L. hemprichii* at the first time point were also identified as core ASVs in the GVC at the second time point, and 90% of core ASVs from the second time point were also identified as core ASVs at the first time point. 68.4% of core ASVs found in the GVC of GBR *L. hemprichii* were also identified as core ASVs in the GVC of aquarium *L. hemprichii*. The 11 ASVs identified as core microbiome in both GBR and aquarium *L. hemprichii* GVC included three Epsilonproteobacteria of the order Campylobacterales, and eight Gammaproteobacteria of the family EC94. Cumulatively, these ASVs represented up to 69.0% of the bacterial relative abundance in GBR *L. hemprichii* GVC at the first sampling point (median = 18.8%), up to 83.0% when resampled (median = 50.0%), and up to 86.7% in the GVC of aquarium *L. hemprichii* (median = 14.3%) (Fig. 6a). None of these ASVs were detected in any other GBR coral or seawater sample, except for a single *L. hemprichii* DBL sample from the GBR (Fig. 6a).

Finally, we used the 16S rDNA sequencing dataset to estimate the abundance of genes that could be considered as markers of aerobic, microaerobic or (facultatively) anaerobic metabolism to investigate the potential of the *L. hemprichii* GVC to host specialised communities. Cumulative abundance of taxa predicted to contain high affinity terminal oxidases (cbb_3 and bd types) was significantly higher in the GVC compared to the DBL and GBR seawater (Fig. 6b. Kruskal-Wallis, χ^2=35.9, P<0.001, followed by Dunn's posthoc test). On the other hand, no significant differences were detected in the predicted abundance of taxa containing low affinity terminal oxidases (aa_3 and bo_3 types. Fig. 6b. Kruskal-Wallis, χ^2=2.27, P=0.32). The median ratio of taxa containing high:low

bioRxiv preprint doi: https://doi.org/10.1101/2024.05.20.594925; this version posted May 20, 2024. The copyright holder for this preprint (which was not certified by peer review) is the author/funder, who has granted bioRxiv a license to display the preprint in perpetuity. It is made available under aCC-BY-NC-ND 4.0 International license.

affinity oxidases fell above 1 for GVC samples, and below 1 for DBL and seawater samples (Fig. 6b). This ratio was significantly different between groups (one-way ANOVA, $F_{2,59}$=3.72, P=0.03), however no individual differences were highlighted by post-hoc testing (Supplementary Table S10). Taxa predicted to contain the anaerobic transcription factor *fnr* were also significantly more abundant in the GVC compared to the DBL and GBR seawater (Fig. 6b. χ^2=32.3, P<0.001). Taxa predicted to contain the gene coding for nitric oxide reductase (*norB*) on the other hand were significantly less abundant in GVC samples compared to DBL and seawater (Supplementary Fig. S8. χ^2=27.9, P<0.001), while those predicted to harbour the catalase gene (*CAT*) were not differentially abundant between compartments (Supplementary Fig. S8, χ^2=0.617, P=0.735).

Discussion

Microscale methods to probe the gastric microbiome of reef corals

We developed and evaluated three different, yet complementary, methods to sample and characterize the gastric microbiome of corals in isolation from other compartments. Our work builds on previous attempts by Agostini et al. [11, 52], who pioneered the glass capillary method to collect gastric fluid from polyps of *G. fascicularis*. One key advancement provided by all our methods was the ability to characterise the gastric microbial community of individual polyps, eliminating the requirement to pool multiple samples in order to obtain sufficient material for molecular analysis. This was not only the case for coral species with large GVCs and large GVC fluid volumes, such as *L. hemprichii*, *F. fungites* and *G. fascicularis*, but also for species with shallower cavities and smaller fluid volumes such as *C. aspera*. Such advancement was made possible by the recent development of a low-input DNA extraction method, which enables recovery of metagenomic-quality DNA from as little as 1 µL of seawater [37]. Our approach now enables in-depth studies focusing on heterogeneity and connectivity of microbial communities at sub-colony and sub-polyp resolution, a knowledge gap previously identified by several studies of microbial diversity in coral holobionts [53–55]. In addition, our approach of sampling corals inside a flow chamber with carefully maintained environmental conditions removes the need for anaesthesia, thus enabling a closer coupling between microbial community characterisation and other physiological measurements such as O_2 dynamics.

Our study introduced two new sampling techniques – extending beyond the glass capillary method – to target the coral gastric microbiome. Using a 34G needle to collect GVC fluid reduces the need for sterilisation of the sampling equipment, as both needles and syringes come pre-sterilised in single-use format. Such type of needle is designed to have minimal dead volume, essential when working with extremely small samples including coral

bioRxiv preprint doi: https://doi.org/10.1101/2024.05.20.594925; this version posted May 20, 2024. The copyright holder for this preprint (which was not certified by peer review) is the author/funder, who has granted bioRxiv a license to display the preprint in perpetuity. It is made available under aCC-BY-NC-ND 4.0 International license.

gastric contents. Furthermore, the seal on the syringe plunger maintains the pressure even when the needle is lowered into or raised from the water, thus eliminating the need for complex equalisation procedures used with the glass capillary (procedures that can also lead to the loss of a small sample volume to prevent contamination). Collectively these characteristics resulted in a more streamlined, faster, and potentially more sterile sampling protocol. Sampling with a nylon microswab on the other hand aimed to target microbial taxa that might be more closely associated with the walls of the GVC, and therefore not necessarily captured when GVC fluid is collected via capillary or needle. Sampling of individual *L. hemprichii* gastric cavities with either the needle or the swab showed a relatively low overlap between bacterial taxa recovered, indicating that the two methods may indeed target different microhabitats within the cavity. However, it is unknown at this point to what extent the two methods may simply bias different microbial taxa, regardless of their location, for example through differential adherence of cells to the nylon swab, or differential release from the swab during DNA extraction [56] – this should be verified in further studies (e.g. by using appropriately constructed mock communities). Compared to the needle method, the swab sampling retrieved more unique ASVs but also more ASVs that were simultaneously detected in the surrounding seawater samples. Seawater contamination is intuitively a more substantial issue in swab samples than in needle samples since the swab is exposed while it travels through water and through the mouth before reaching the gastric cavity. To limit this issue, we recommend lowering the water level in the flow chamber as much as possible immediately prior to sampling, as even leaving the coral surface shortly exposed did not hinder insertion of the swab. We also recommend choosing carefully between the two methods depending on the specific research question, and potentially using both methods in conjunction for a more complete characterisation of the coral gastric microbiome.

Oxygen in the coral gastric cavity: a gut-like environment?

Our characterisation of the O_2 environment inside coral GVCs revealed some similarities between species. With the exception of *F. fungites*, all species examined presented an upper cavity environment that was generally hyperoxic in the light and normoxic or hypoxic in darkness. These characteristics are consistent with what is commonly observed in the diffusive boundary layer of corals during a diel cycle [38, 57–59]. Moving deeper into the cavity, hypoxic or anoxic regions persisted even under saturating illumination in many of the coral polyps examined. Our study thus confirms that hypoxic micro-niches, previously detected in the *G. fascicularis* GVC [11], exist in the GVC of a range of coral species. A persistently anoxic or hypoxic environment is a key feature of the digestive tract of higher metazoans including the vertebrate gut [60–63]. In fact, the combination of an

bioRxiv preprint doi: https://doi.org/10.1101/2024.05.20.594925; this version posted May 20, 2024. The copyright holder for this preprint (which was not certified by peer review) is the author/funder, who has granted bioRxiv a license to display the preprint in perpetuity. It is made available under aCC-BY-NC-ND 4.0 International license.

anaerobic environment with a high supply of sugar is thought to be one of the factors contributing to shape gut differentiation across the tree of life [63]. Hypoxic guts support specialised microbial communities, which in many organisms contribute to the wellbeing of the host by making undigestible compounds bioavailable (termite guts represent an extreme example; [60]), by producing key metabolites (e.g. vitamins), and by defending against pathogens via antimicrobial activity [64–66]. Thus, the existence of a gut-like chemical environment in corals calls for further exploration of the microbial complement that inhabits it, and of the role these communities may play in holobiont ecophysiology.

A time series of O_2 concentration inside the *L. hemprichii* GVC revealed that light is not the only factor shaping oxygen distribution in the GVC. Under prolonged darkness, oxygen concentrations in the GVC fluctuated from anoxic to normoxic. As no production of oxygen occurred through photosynthesis, these fluctuations were most likely due to water exchange between the hypoxic/anoxic GVC and the surrounding oxygenated seawater, possibly caused by contraction and expansion movements of the tissue that create a ventilation effect. Therefore, at least for some coral species, polyp behaviour may play a role in controlling the chemical environment of the GVC and, indirectly, the microbial community that inhabits it. The normoxic, relatively homogeneous oxygen environment of the *F. fungites* GVC could also be explained by a process of ventilation, which may be more effective in corals with larger polyps. Probing the GVC under conditions that affect tissue contraction, such as anaesthesia, stress or feeding will reveal to what extent coral polyps can regulate their GVC oxygen environment.

The gastric microbiome of corals

Metabarcoding of microbial communities found in the DBL and GVC of GBR corals via 16S rDNA sequencing revealed that these communities are different from each other, and that they are also distinct from the surrounding seawater. While communities found in the DBL were similar to each other and similar to those found in seawater, communities sampled from coral GVCs had much wider dispersion, with some samples appearing very different not only from water samples, but also from other GVC samples. Over 50% of GVC samples from multiple species on the other hand appeared to host communities closer to the DBL and SW in composition – this was the case particularly for *D. favus*, *F. pentagona* and *C. aspera*. It is possible that potential contamination with the surrounding seawater masks the GVC community signal for certain samples only. However, it is also plausible this dispersion could result from true biological variability, whereby the GVCs of some polyps host more specialised communities while others are dominated by transient taxa found in seawater. Differences in the rate

bioRxiv preprint doi: https://doi.org/10.1101/2024.05.20.594925; this version posted May 20, 2024. The copyright holder for this preprint (which was not certified by peer review) is the author/funder, who has granted bioRxiv a license to display the preprint in perpetuity. It is made available under aCC-BY-NC-ND 4.0 International license.

of GVC ventilation through polyp contraction, as described for *L. hemprichii*, could lead to some polyps having more extensive mixing with the surrounding environment, and therefore a microbiome that more closely resembles that of seawater or the DBL.

Intercolonial variability in microbial community composition is common across many coral taxa [67, 68], and intracolonial heterogeneity has also been previously reported when bulk sampling (i.e. combining tissue, mucus, skeleton in a single sample) [54, 69] or sampling specific compartments [53], although contrasting reports also exist [70]. Thus, GVC microbial communities found in polyps of the same species or even within the same colony could have very different composition, perhaps driven by polyp age, size, position within the colony, or recent feeding activities. Whilst this question cannot be resolved with our current dataset, the methods developed in this study are ideally suited for further investigations in this direction. Nonetheless, our data show that, at least for 30-50% of individual polyps, the GVC of all investigated GBR species hosts a microbial community that is distinct from that encountered in the surrounding seawater. The polyps with the most compositionally distinct GVC communities also exhibited lower diversity compared to the communities found in seawater. Such a notion is consistent with the observation that animal-associated microbial communities tend to have lower diversity than those found in the environment immediately surrounding them [6], and resembles what has been reported for the gut microbiome of other invertebrates, such as insects [71]. While reduced microbial diversity is an expected result in an invertebrate "gut" environment, the total number of bacterial cells retrieved from our coral GVC samples was often very similar to the cell densities recorded in seawater. This result is in contrast with a previous observation reporting two orders of magnitude more cells in the *G. fascicularis* gastric fluid compared to the surrounding seawater [11].

Metabarcoding of microbial communities found in the coral GVC highlighted a few taxa of interest. Epsilonproteobacteria (formerly Campylobacteria) were highly abundant in at least some of the GVC samples collected from all GBR coral species examined here (with the exception of *D. favus*). This group was particularly abundant in the GVC of *L. hemprichii*, including in aquarium colonies with a diverse environmental history, and some taxa of the order Campylobacterales were identified as part of the *L. hemprichii* core gastric microbiome. Epsilonproteobacteria are a class of Proteobacteria which includes many microaerophilic taxa, including known gut symbionts of other marine invertebrates [72–75], as well as mammalian gut commensals and/or pathogens [76]. Thanks to the ability of some taxa in this group to obtain energy from the oxidation of reduced compounds

bioRxiv preprint doi: https://doi.org/10.1101/2024.05.20.594925; this version posted May 20, 2024. The copyright holder for this preprint (which was not certified by peer review) is the author/funder, who has granted bioRxiv a license to display the preprint in perpetuity. It is made available under aCC-BY-NC-ND 4.0 International license.

(chemolithotrophy) Epsilonproteobacteria dominate marine communities in sulfide-rich or hydrocarbon-rich environments, such as hydrothermal vents and sediment [76], and some taxa have become symbionts of hydrothermal vent invertebrates [77]. In corals, Epsilonproteobacteria have been previously identified as abundant taxa in tissue affected by disease or bleaching [78–81]. The presence of microaerophilic, potentially chemolithotrophic taxa in the coral gastric cavity further likens this compartment to a true animal gut, especially since some of these taxa appear to associate non-transiently with *L. hemprichii*. This discovery calls for a more in-depth investigation into the metabolism of coral gut-associated Epsilonproteobacteria to identify (i) which electron acceptors (e.g. oxygen, nitrate or sulfate) and electron donors (e.g. sulfide, thiosulfate, hydrogen) they predominantly utilise [82], and (ii) which holobiont members and physiological processes could be the source of these chemicals.

One Epsilonprotebacteria ASV found in high abundance almost exclusively in the GVC of *L. hemprichii* from the GBR was identified as *Thiovulum* sp. Members of this genus include large, highly motile sulfur-oxidising bacteria, commonly found at sulfide/oxygen interfaces where they sometimes form thick veils [83, 84]. As these cells require both oxygen and sulfide, they tend to congregate around 4% O_2 saturation, and they are able to position themselves within the oxygen gradient via chemotaxis [84, 85]. The lower portion of the *L. hemprichii* GVC presents the ideal oxygen environment for *Thiovulum*, since this region remains hypoxic even in the light. However, a question remains regarding the potential presence and origin of sulfide in the anoxic cavity bottom, which to our knowledge has never been investigated. Sulfide production in corals has so far only been detected with microsensors under prolonged anoxic conditions, such as those that develop during exposure to organic-rich sediment [86] or infection with black band disease [87]. A similar approach could be applied to investigate the production of sulfide as well as other potential electron donors, such as hydrogen, in the GVC of healthy corals.

A second group which was more abundant in coral samples (both DBL and GVC, except for the *G. fascicularis* GVC and the *L. hemprichii* DBL) compared to seawater, and particularly abundant in the *L. hemprichii* GVC, was Anaerolineae. These are a class of Chloroflexota often isolated from microaerophilic or anoxic environments such as anaerobic digesters [88] and the mammalian gut [89], but they are also sometimes found in healthy coral tissue [81] as well as sponges [90]. This group was also reported to be enriched in seawater containing coral mucus [91]. While we cannot infer the metabolism of the specific taxa identified here simply from their taxonomic assignment,

bioRxiv preprint doi: https://doi.org/10.1101/2024.05.20.594925; this version posted May 20, 2024. The copyright holder for this preprint (which was not certified by peer review) is the author/funder, who has granted bioRxiv a license to display the preprint in perpetuity. It is made available under aCC-BY-NC-ND 4.0 International license.

554 their potential involvement in fermentative pathways in the GVC is an intriguing possibility, which could have
555 implications for digestion and resource assimilation by the holobiont.
556
557 Lastly, ASVs belonging to the family EC94 were enriched in the *L. hemprichii* GVC on the GBR, while absent
558 from most other samples other than the GVC of *F. pentagona*. Some of these ASVs were also found in high
559 abundance in the GVC of *L. hemprichii* from long-term aquarium culture, and were thus deemed to constitute part
560 of the core *L. hemprichii* gastric microbiome. EC94 is a relatively uncharacterized group of marine Proteobacteria,
561 which are predominantly associated with sponges, recently proposed for reclassification as the order Ca.
562 Tethybacterales [92]. While members of this group are not very broadly encountered in coral samples, they appear
563 to be dominant/core symbionts for a few coral species, including *Agaricia undata* in the Caribbean [93], *Mycedium*
564 *elephantotus* in the Indo-Pacific [94], and now *L. hemprichii* on the GBR. In sponges, Ca. Tethybacterales exhibit
565 diverse morphology and distribution, and often reside within specialized cells (bacteriocytes) [92]. Metagenome-
566 assembled genomes (MAGs) for this group indicate they are likely aerobic or microaerophilic heterotrophs
567 capable of utilizing a range of carbon, nitrogen and sulfur sources including dimethylsulfoniopropionate (DMSP)
568 and glycine betaine [92], both of which are highly abundant in symbiotic corals [95].
569
570 Interestingly, we only detected low abundance of *Endozoicomonas* in the GVC of most GBR species investigated.
571 *Endozoicomonas* are a genus of Gammaproteobacteria known to be prevalent and abundant in many coral species
572 [96], often found as microbial aggregates (CAMAs) within the host tissue together with *Simkania* [51] – another
573 taxon that was largely absent from our dataset. *Endozoicomonas* were also completely absent from aquarium *L.*
574 *hemprichii* colonies, consistent with the common observation that *Endozoicomonas* are lost in captivity [97]. Since
575 we did not sample the tissue directly, we cannot exclude that these corals had naturally low concentrations of
576 these bacteria, as has been sometimes reported for corals from other locations [98]. Nonetheless, our data show
577 that low concentrations of CAMA-forming bacteria are present also in the coral GVC, which could constitute a
578 point of entry and exit for these microorganisms. Other potential sources of *Endozoicomonas* in the GVC include
579 ingestion and contamination from the tissue, or resident CAMAs could exist in the GVC of corals, similarly to
580 what observed in the gills of bivalves [99].
581
582 Alongside differential abundance and core microbiome analysis, we investigated the metabolic potential of the *L.*
583 *hemprichii* and seawater microbial communities by generating predicted metagenomes and interrogating them for

bioRxiv preprint doi: https://doi.org/10.1101/2024.05.20.594925; this version posted May 20, 2024. The copyright holder for this preprint (which was not certified by peer review) is the author/funder, who has granted bioRxiv a license to display the preprint in perpetuity. It is made available under aCC-BY-NC-ND 4.0 International license.

584 the presence of a set of marker genes [47, 50]. The genes coding for the terminal oxidases of respiratory chains
585 can provide insights into the oxygen requirements of organisms [100]. Low affinity terminal oxidases include the
586 aa_3 and bo_3 types, which are found in obligate aerobes and facultative anaerobes. The cbb_3 and bd types on the
587 other hand have a higher affinity for oxygen, thus they allow organisms to survive in low-oxygen environments
588 (microaerophiles and some facultative anaerobes) [100]. Our analysis predicted that high affinity oxidases in the
589 GVC of *L. hemprichii* could be (i) more abundant than low affinity ones, and (ii) more abundant than in the DBL
590 or seawater. This suggests that the GVC may harbour a community enriched in microaerophilic and facultatively
591 anaerobic taxa, a prediction consistent with the presence of hypoxic and anoxic zones in the lower GVC as
592 detected by our oxygen microsensor measurements. In addition, we predicted higher abundance in the GVC for
593 the anaerobic transcription factor gene *fnr*, which regulates the switch to anaerobic pathways in facultative
594 anaerobes such as *E. coli* [101]. While this type of analysis is simply a prediction, if validated by metagenomic
595 data it would provide a strong parallel with other animal gut microbiomes. High affinity terminal oxidases are the
596 dominant (or exclusive) terminal oxidases in many vertebrate guts [100], including healthy humans [102].
597 Conversely, high affinity oxidases are much less abundant in environmental metagenomes, including both
598 terrestrial and marine communities [100]. High affinity terminal oxidases are also widespread in arthropod gut
599 microbiomes [103], including the microoxic/anoxic hindgut of termites [104].
600
601 Interestingly, the nitric oxide reductase encoding gene *norB* was predicted to be less abundant in GVC
602 communities compared to DBL and seawater. If this prediction were to be supported with metagenomic data, it
603 would indicate lower abundance of (facultatively) anaerobic taxa that rely on nitrate as alternative electron
604 acceptor [49, 105]. The antioxidant enzyme catalase (*CAT*) is often used as an indicator for aerobic or oxygen
605 tolerant species [106], as its role in detoxification of reactive oxygen species is key to survival in a high oxygen
606 environment (however, note that some strict anaerobes also possess catalase genes [107]). We found no difference
607 in the predicted abundance of this gene between the GVC, the DBL and seawater. We hypothesise that most taxa
608 residing in the GVC should be able to at least tolerate oxygen, given their immediate proximity to the
609 photosynthetic endosymbionts harboured in the coral gastrodermal tissue and given the potential ventilation
610 occurring due to tissue contractions, which result in a highly dynamic oxygen environment. We note that
611 predicting metagenomes from metabarcoding data can often yield misleading results due to the scarcity of
612 annotated genomes for many bacterial taxa, as well as pervasive horizontal gene transfer occurring in microbial
613 communities [108, 109]. However, the predicted abundance of markers *fnr*, *norB* and *CAT* has been previously

bioRxiv preprint doi: https://doi.org/10.1101/2024.05.20.594925; this version posted May 20, 2024. The copyright holder for this preprint (which was not certified by peer review) is the author/funder, who has granted bioRxiv a license to display the preprint in perpetuity. It is made available under aCC-BY-NC-ND 4.0 International license.

614 shown to correlate well with metagenomic data [50]. These predictions can thus constitute a useful starting point
615 for hypothesis generation, and can be used to guide future investigations.
616
617 **Conclusion**
618 Multiple lines of evidence presented here highlight similarities between the coral GVC and the guts of higher
619 vertebrates and invertebrates. The GVC contains permanently hypoxic and anoxic regions, and hosts a distinct
620 microbial community compared to the surrounding seawater environment. The GVC community is lower in
621 diversity and enriched in putatively anaerobic and microaerophilic taxa, including relatives of the gut microbiota
622 of other animals. In *L. hemprichii* (the species we studied in greater detail), some of these taxa appear to form a
623 core community which is conserved in conspecifics from different locations, and which persists after long-term
624 aquarium culture. The microscale methods described in this article will enable further studies into the functional
625 profiles of these communities, for example via metagenomics or metatranscriptomics, shedding light on the role
626 played by the GVC microbiome in the physiology of the coral holobiont. We hope that these methods will pave
627 the way towards developing "coral gut microbiology" as a new field within the broader domain of coral
628 ecophysiological research. We anticipate that that this effort will help identify pathways and interactions within
629 the holobiont as suitable potential targets for manipulative intervention, and eventually contribute to increasing
630 the resilience of corals to climate change.
631
632 **Funding**
633 This study was supported by a grant from the Gordon and Betty Moore Foundation (grant no. GBMF9206;
634 https://doi.org/10.37807/GBMF9206) to MK.
635
636 **Author contributions**
637 All authors contributed to the study design. MK obtained funding. EB, DJH and JBR performed the experiments
638 and analysed the data. EB and DJH wrote the first draft of the manuscript. All authors edited and contributed to
639 subsequent manuscript drafts.
640
641 **Acknowledgements**
642 We thank the staff at Heron Island Research Station for assistance during the field work, and the Great Barrier
643 Reef Marine Parks authority for enabling our fieldwork under permit no. G18/41633.1. Caitlin Lawson for help

bioRxiv preprint doi: https://doi.org/10.1101/2024.05.20.594925; this version posted May 20, 2024. The copyright holder for this preprint (which was not certified by peer review) is the author/funder, who has granted bioRxiv a license to display the preprint in perpetuity. It is made available under aCC-BY-NC-ND 4.0 International license.

644 with coral collection on Heron Island. Deepa Varkey for assistance with preliminary data analysis. Natasha
645 Bartels, Hadley England, Kieran Chau, Nicole Dilernia and Emma Camp provided assistance with aquarium work
646 and materials at UTS. Anna Bramucci and Trent Haydon helped with laboratory procedures at UTS.

647

648 **Competing Interests**

649 The authors declare no competing interests.

650

651 **Data availability**

652 All raw sequencing data has been deposited to SRA (PRJNA1074944). The remaining raw data is available from
653 Dryad (doi:10.5061/dryad.p5hqbzkwj).

bioRxiv preprint doi: https://doi.org/10.1101/2024.05.20.594925; this version posted May 20, 2024. The copyright holder for this preprint (which was not certified by peer review) is the author/funder, who has granted bioRxiv a license to display the preprint in perpetuity. It is made available under aCC-BY-NC-ND 4.0 International license.

654 **References**

655 1. Ley RE, Peterson DA, Gordon JI. Ecological and evolutionary forces shaping
656 microbial diversity in the human intestine. *Cell* 2006; **124**: 837–848.
657 2. Wu H-J, Wu E. The role of gut microbiota in immune homeostasis and autoimmunity.
658 *Gut Microbes* 2012; **3**: 4–14.
659 3. Forssten SD, Ouwehand AC, Griffin SM, Patterson E. One giant leap from mouse to
660 man: The microbiota–gut–brain axis in mood disorders and translational challenges
661 moving towards human clinical trials. *Nutrients* 2022; **14**: 568.
662 4. Yoon SS, Kim EK, Lee WJ. Functional genomic and metagenomic approaches to
663 understanding gut microbiota-animal mutualism. *Curr Opin Microbiol* 2015; **24**: 38–
664 46.
665 5. Ludington WB, Ja WW. Drosophila as a model for the gut microbiome. *PLOS Pathog*
666 2020; **16**: e1008398.
667 6. Boscaro V, Holt CC, Van Steenkiste NWL, Herranz M, Irwin NAT, Àlvarez-Campos
668 P, et al. Microbiomes of microscopic marine invertebrates do not reveal signatures of
669 phylosymbiosis. *Nat Microbiol* 2022; **7**: 810–819.
670 7. Hughes DJ, Raina J-B, Nielsen DA, Suggett DJ, Kühl M. Disentangling compartment
671 functions in sessile marine invertebrates. *Trends Ecol Evol* 2022.
672 8. van Oppen MJH, Raina J-B. Coral holobiont research needs spatial analyses at the
673 microbial scale. *Environ Microbiol* 2023; **25**: 179–183.
674 9. Muscatine L. The role of symbiotic algae in carbon and energy flux in coral reefs. In:
675 Dubinsky Z (ed). *Ecosystems of the World, 25. Coral Reefs*. 1990. Elsevier,
676 Amsterdam, pp 75–87.
677 10. Raz-Bahat M, Douek J, Moiseeva E, Peters EC, Rinkevich B. The digestive system of
678 the stony coral *Stylophora pistillata*. *Cell Tissue Res* 2017; **368**: 311–323.

bioRxiv preprint doi: https://doi.org/10.1101/2024.05.20.594925; this version posted May 20, 2024. The copyright holder for this preprint (which was not certified by peer review) is the author/funder, who has granted bioRxiv a license to display the preprint in perpetuity. It is made available under aCC-BY-NC-ND 4.0 International license.

679 11. Agostini S, Suzuki Y, Higuchi T, Casareto BE, Yoshinaga K, Nakano Y, et al.
680 Biological and chemical characteristics of the coral gastric cavity. *Coral Reefs* 2012;
681 **31**: 147–156.
682 12. Bove CB, Whitehead RF, Szmant AM. Responses of coral gastrovascular cavity pH
683 during light and dark incubations to reduced seawater pH suggest species-specific
684 responses to the effects of ocean acidification on calcification. *Coral Reefs* 2020; **39**:
685 1675–1691.
686 13. Jokic T, Borisov SM, Saf R, Nielsen DA, Kühl M, Klimant I. Highly photostable near-
687 infrared fluorescent pH indicators and sensors based on BF2-chelated
688 tetraarylazadipyrromethene dyes. *Anal Chem* 2012; **84**: 6723–6730.
689 14. Yuan X, Cai WJ, Meile C, Hopkinson BM, Ding Q, Schoepf V, et al. Quantitative
690 interpretation of vertical profiles of calcium and pH in the coral coelenteron. *Mar*
691 *Chem* 2018; **204**: 62–69.
692 15. Bourne DG, Morrow KM, Webster NS. Insights into the coral microbiome:
693 underpinning the health and resilience of reef ecosystems. *Annu Rev Microbiol* 2016;
694 **70**: 317–340.
695 16. Peixoto RS, Sweet M, Villela HDM, Cardoso P, Thomas T, Voolstra CR, et al. Coral
696 probiotics: Premise, promise, prospects. *Annu Rev Anim Biosci* 2021; **9**: 265–288.
697 17. Hoegh-Guldberg O, Skirving W, Dove SG, Spady BL, Norrie A, Geiger EF, et al.
698 Coral reefs in peril in a record-breaking year. *Science* 2023; **382**: 1238–1240.
699 18. Voolstra CR, Suggett DJ, Peixoto RS, Parkinson JE, Quigley KM, Silveira CB, et al.
700 Extending the natural adaptive capacity of coral holobionts. *Nat Rev Earth Environ*
701 2021; **2**: 747–762.

bioRxiv preprint doi: https://doi.org/10.1101/2024.05.20.594925; this version posted May 20, 2024. The copyright holder for this preprint (which was not certified by peer review) is the author/funder, who has granted bioRxiv a license to display the preprint in perpetuity. It is made available under aCC-BY-NC-ND 4.0 International license.

19. Rosado PM, Leite DCA, Duarte GAS, Chaloub RM, Jospin G, Nunes da Rocha U, et al. Marine probiotics: increasing coral resistance to bleaching through microbiome manipulation. *ISME J* 2019; **13**: 921–936.

20. Santoro EP, Borges RM, Espinoza JL, Freire M, Messias CSMA, Villela HDM, et al. Coral microbiome manipulation elicits metabolic and genetic restructuring to mitigate heat stress and evade mortality. *Sci Adv* 2021; **7**: 19–21.

21. Garcias-Bonet N, Roik A, Tierney B, García FC, Villela HDM, Dungan AM, et al. Horizon scanning the application of probiotics for wildlife. *Trends Microbiol* 2023; **0**.

22. Li J, Zou Y, Li Q, Zhang J, Bourne DG, Lyu Y, et al. A coral-associated actinobacterium mitigates coral bleaching under heat stress. *Environ Microbiome* 2023; **18**: 83.

23. Moradi M, Magalhaes PR, Peixoto RS, Jonck CCAC, François D, Bellot ACF, et al. Probiotics mitigate thermal stress- and pathogen-driven impacts on coral skeleton. *Front Mar Sci* 2023; **10**.

24. Rosado PM, Cardoso PM, Rosado JG, Schultz J, Nunes da Rocha U, Keller-Costa T, et al. Exploring the potential molecular mechanisms of interactions between a probioticcConsortium and its coral host. *mSystems* 2023.

25. Shashar N, Cohen Y, Loya Y, Sar N. Nitrogen fixation (acetylene reduction) in stony corals: evidence for coral-bacteria interactions. *Mar Ecol Prog Ser* 1994; **111**: 259–264.

26. Tandon K, Lu C-Y, Chiang P-W, Wada N, Yang S-H, Chan Y-F, et al. Comparative genomics: Dominant coral-bacterium *Endozoicomonas acroporae* metabolizes dimethylsulfoniopropionate (DMSP). *ISME J* 2020; **14**: 1290–1303.

bioRxiv preprint doi: https://doi.org/10.1101/2024.05.20.594925; this version posted May 20, 2024. The copyright holder for this preprint (which was not certified by peer review) is the author/funder, who has granted bioRxiv a license to display the preprint in perpetuity. It is made available under aCC-BY-NC-ND 4.0 International license.

725 27. Pogoreutz C, Oakley CA, Rädecker N, Cárdenas A, Perna G, Xiang N, et al. Coral
726 holobiont cues prime *Endozoicomonas* for a symbiotic lifestyle. *ISME J* 2022; **16**:
727 1883–1895.
728 28. Matthews JL, Khalil A, Siboni N, Bougoure J, Guagliardo P, Kuzhiumparambil U, et
729 al. Coral endosymbiont growth is enhanced by metabolic interactions with bacteria.
730 *Nat Commun* 2023; **14**: 1–13.
731 29. Marangon E, Laffy PW, Bourne DG, Webster NS. Microbiome - mediated
732 mechanisms contributing to the environmental tolerance of reef invertebrate species.
733 *Mar Biol* 2021; 1–18.
734 30. Apprill A, Weber LG, Santoro AE. Distinguishing between microbial habitats unravels
735 ecological complexity in coral microbiomes. *mSystems* 2016; **1**.
736 31. Pollock FJ, McMinds R, Smith S, Bourne DG, Willis BL, Medina M, et al. Coral-
737 associated bacteria demonstrate phylosymbiosis and cophylogeny. *Nat Commun* 2018;
738 **9**.
739 32. Biagi E, Caroselli E, Barone M, Pezzimenti M, Teixido N, Soverini M, et al. Patterns
740 in microbiome composition differ with ocean acidification in anatomic compartments
741 of the Mediterranean coral *Astroides calycularis* living at CO_2 vents. *Sci Total Environ*
742 2020; **724**.
743 33. Marchioro GM, Glasl B, Engelen AH, Serrão EA, Bourne DG, Webster NS, et al.
744 Microbiome dynamics in the tissue and mucus of acroporid corals differ in relation to
745 host and environmental parameters. *PeerJ* 2020; **8**.
746 34. Sweet MJ, Croquer A, Bythell JC. Bacterial assemblages differ between compartments
747 within the coral holobiont. *Coral Reefs* 2011; **30**: 39–52.

bioRxiv preprint doi: https://doi.org/10.1101/2024.05.20.594925; this version posted May 20, 2024. The copyright holder for this preprint (which was not certified by peer review) is the author/funder, who has granted bioRxiv a license to display the preprint in perpetuity. It is made available under aCC-BY-NC-ND 4.0 International license.

748 35. Ainsworth TD, Krause L, Bridge T, Torda G, Raina JB, Zakrzewski M, et al. The coral
749 core microbiome identifies rare bacterial taxa as ubiquitous endosymbionts. *ISME J*
750 2015; **9**: 2261–2274.
751 36. Tang K, Zhan W, Zhou Y, Xu T, Chen X, Wang W, et al. Antagonism between coral
752 pathogen *Vibrio coralliilyticus* and other bacteria in the gastric cavity of scleractinian
753 coral *Galaxea fascicularis*. *Sci China Earth Sci* 2020; **63**: 157–166.
754 37. Bramucci AR, Focardi A, Rinke C, Hugenholtz P, Tyson GW, Seymour JR, et al.
755 Microvolume DNA extraction methods for microscale amplicon and metagenomic
756 studies. *ISME Commun* 2021; **1**: 79.
757 38. Kühl M, Cohen Y, Dalsgaard T, Jorgensen BB, Revsbech NP. Microenvironment and
758 photosynthesis of zooxanthellae in scleractinian corals studied with microsensors for
759 0_2, pH and light. *Mar Ecol Prog Ser* 1995; **117**: 159-172.1995.
760 39. Marie D, Partensky F, Jacquet S, Vaulot D. Enumeration and cell cycle analysis of
761 natural populations of marine picoplankton by flow cytometry using the nucleic acid
762 stain SYBR Green I. *Appl Environ Microbiol* 1997; **63**: 186–193.
763 40. Martin M. Cutadapt removes adapter sequences from high-throughput sequencing
764 reads. *EMBnet.journal* 2011; **17**: 10–12.
765 41. Callahan BJ, McMurdie PJ, Rosen MJ, Han AW, Johnson AJA, Holmes SP. DADA2:
766 High-resolution sample inference from Illumina amplicon data. *Nat Methods* 2016; **13**:
767 581–583.
768 42. Quast C, Pruesse E, Yilmaz P, Gerken J, Schweer T, Yarza P, et al. The SILVA
769 ribosomal RNA gene database project: Improved data processing and web-based tools.
770 *Nucleic Acids Res* 2013; **41**.
771 43. Oksanen J, Simpson GL, Blanchet FG, Kindt R, Legendre P, Minchin PR, et al. vegan:
772 Community Ecology Package. 2022.

bioRxiv preprint doi: https://doi.org/10.1101/2024.05.20.594925; this version posted May 20, 2024. The copyright holder for this preprint (which was not certified by peer review) is the author/funder, who has granted bioRxiv a license to display the preprint in perpetuity. It is made available under aCC-BY-NC-ND 4.0 International license.

773 44. McMurdie PJ, Holmes S. Phyloseq: An R package for reproducible interactive analysis
774 and graphics of microbiome census data. *PLoS ONE* 2013; **8**.
775 45. Fernandes AD, Macklaim JM, Linn TG, Reid G, Gloor GB. ANOVA-Like Differential
776 Expression (ALDEx) analysis for mixed population RNA-Seq. *PLOS ONE* 2013; **8**:
777 e67019.
778 46. Lathi L, Shetty S. microbiome R package. 2012.
779 47. Douglas GM, Maffei VJ, Zaneveld JR, Yurgel SN, Brown JR, Taylor CM, et al.
780 PICRUSt2 for prediction of metagenome functions. *Nat Biotechnol* 2020; **38**: 685–688.
781 48. Kanehisa M, Goto S, Sato Y, Furumichi M, Tanabe M. KEGG for integration and
782 interpretation of large-scale molecular data sets. *Nucleic Acids Res* 2012; **40**: D109–
783 D114.
784 49. Sousa FL, Nelson-Sathi S, Martin WF. One step beyond a ribosome: The ancient
785 anaerobic core. *Biochim Biophys Acta* 2016; **1857**: 1027–1038.
786 50. Epihov DZ, Saltonstall K, Batterman SA, Hedin LO, Hall JS, Van Breugel M, et al.
787 Legume–microbiome interactions unlock mineral nutrients in regrowing tropical
788 forests. *Proc Natl Acad Sci* 2021; **118**: e2022241118.
789 51. Maire J, Tandon K, Collingro A, van de Meene A, Damjanovic K, Gotze CR, et al.
790 Colocalization and potential interactions of *Endozoicomonas* and Chlamydiae in
791 microbial aggregates of the coral *Pocillopora acuta*. *Sci Adv* 2023; **9**: eadg0773.
792 52. Agostini S, Suzuki Y, Casareto BE, Nakano Y, Fairoz MFM, Shiroma K, et al. New
793 approach to study the coral symbiotic complex: Application to vitamin B 12. 2008.
794 53. Daniels CA, Zeifman A, Heym K, Ritchie KB, Watson CA, Berzins I, et al. Spatial
795 heterogeneity of bacterial communities in the mucus of *Montastraea annularis*. *Mar*
796 *Ecol Prog Ser* 2011; **426**: 29–40.

bioRxiv preprint doi: https://doi.org/10.1101/2024.05.20.594925; this version posted May 20, 2024. The copyright holder for this preprint (which was not certified by peer review) is the author/funder, who has granted bioRxiv a license to display the preprint in perpetuity. It is made available under aCC-BY-NC-ND 4.0 International license.

797 54. Damjanovic K, Blackall LL, Peplow LM, van Oppen MJH. Assessment of bacterial
798 community composition within and among *Acropora loripes* colonies in the wild and
799 in captivity. *Coral Reefs* 2020; **39**: 1245–1255.
800 55. Bergman JL, Shaw T, Egan S, Ainsworth TD. Assessing the coral microbiome at the
801 scale of tissue-specific habitats within the coral meta-organism. *Front Mar Sci* 2022; **9**.
802 56. Motz VA, Young LM, Motz ME, Young SC. A sticking point in assessing bacterial
803 contamination: Adhesive characters of bacterial specializations, swab features, and
804 fomite surface properties skew colony counts. *J Pure Appl Microbiol* 2019; **13**.
805 57. Shashar N, Cohen Y, Loya Y. Extreme diel fluctuations of oxygen in diffusive
806 boundary layers surrounding stony corals. *Biol Bull* 1993; **185**: 455–461.
807 58. Linsmayer LB, Deheyn DD, Tomanek L, Tresguerres M. Dynamic regulation of coral
808 energy metabolism throughout the diel cycle. *Sci Rep* 2020; **10**: 1–11.
809 59. Pacherres CO, Ahmerkamp S, Schmidt-Grieb GM, Holtappels M, Richter C. Ciliary
810 vortex flows and oxygen dynamics in the coral boundary layer. *Sci Rep* 2020; **10**:
811 7541.
812 60. Brune A. Termite guts: the world's smallest bioreactors. *Trends Biotechnol* 1998; **16**:
813 16–21.
814 61. Stief P, Eller G. The gut microenvironment of sediment-dwelling *Chironomus*
815 *plumosus* larvae as characterised with O_2, pH, and redox microsensors. *J Comp Physiol*
816 *B* 2006; **176**: 673–683.
817 62. Tegtmeier D, Thompson CL, Schauer C, Brune A. Oxygen affects gut bacterial
818 colonization and metabolic activities in a gnotobiotic cockroach model. *Appl Environ*
819 *Microbiol* 2016; **82**: 1080–1089.

bioRxiv preprint doi: https://doi.org/10.1101/2024.05.20.594925; this version posted May 20, 2024. The copyright holder for this preprint (which was not certified by peer review) is the author/funder, who has granted bioRxiv a license to display the preprint in perpetuity. It is made available under aCC-BY-NC-ND 4.0 International license.

820 63. Friedman ES, Bittinger K, Esipova TV, Hou L, Chau L, Jiang J, et al. Microbes vs.
821 chemistry in the origin of the anaerobic gut lumen. *Proc Natl Acad Sci* 2018; **115**:
822 4170–4175.
823 64. Nicholson JK, Holmes E, Kinross J, Burcelin R, Gibson G, Jia W, et al. Host-gut
824 microbiota metabolic interactions. *Science* 2012; **336**: 1262–1267.
825 65. LeBlanc JG, Milani C, de Giori GS, Sesma F, van Sinderen D, Ventura M. Bacteria as
826 vitamin suppliers to their host: a gut microbiota perspective. *Curr Opin Biotechnol*
827 2013; **24**: 160–168.
828 66. Agamennone V, Le NG, van Straalen NM, Brouwer A, Roelofs D. Antimicrobial
829 activity and carbohydrate metabolism in the bacterial metagenome of the soil-living
830 invertebrate *Folsomia candida*. *Sci Rep* 2019; **9**: 7308.
831 67. Glasl B, Smith CE, Bourne DG, Webster NS. Disentangling the effect of host-
832 genotype and environment on the microbiome of the coral *Acropora tenuis*. *PeerJ*
833 2019; **7**: e6377.
834 68. Kanisan DP, Quek ZBR, Oh RM, Afiq-Rosli L, Lee JN, Huang D, et al. Diversity and
835 distribution of microbial communities associated with reef corals of the Malay
836 peninsula. *Microb Ecol* 2023; **85**: 37–48.
837 69. Rohwer F, Seguritan V, Azam F, Knowlton N. Diversity and distribution of coral-
838 associated bacteria. *Mar Ecol Prog Ser* 2002; **243**: 1–10.
839 70. Kemp DW, Rivers AR, Kemp KM, Lipp EK, Porter JW, Wares JP. Spatial
840 homogeneity of bacterial communities associated with the surface mucus layer of the
841 reef-building coral *Acropora palmata*. *PLOS ONE* 2015; **10**: e0143790.
842 71. Yun JH, Roh SW, Whon TW, Jung MJ, Kim MS, Park DS, et al. Insect gut bacterial
843 diversity determined by environmental habitat, diet, developmental stage, and
844 phylogeny of host. *Appl Environ Microbiol* 2014; **80**: 5254–5264.

bioRxiv preprint doi: https://doi.org/10.1101/2024.05.20.594925; this version posted May 20, 2024. The copyright holder for this preprint (which was not certified by peer review) is the author/funder, who has granted bioRxiv a license to display the preprint in perpetuity. It is made available under aCC-BY-NC-ND 4.0 International license.

845 72. Tanaka R, Ootsubo M, Sawabe T, Ezura Y, Tajima K. Biodiversity and in situ
846 abundance of gut microflora of abalone (*Haliotis discus hannai*) determined by
847 culture-independent techniques. *Aquaculture* 2004; **241**: 453–463.
848 73. Corbari L, Durand L, Cambon-Bonavita M-A, Gaill F, Compère P. New digestive
849 symbiosis in the hydrothermal vent amphipoda *Ventiella sulfuris*. *C R Biol* 2012; **335**:
850 142–154.
851 74. Hakim JA, Koo H, Dennis LN, Kumar R, Ptacek T, Morrow CD, et al. An abundance
852 of Epsilonproteobacteria revealed in the gut microbiome of the laboratory cultured sea
853 urchin, *Lytechinus variegatus*. *Front Microbiol* 2015; **6**.
854 75. Weigel BL. Sea cucumber intestinal regeneration reveals deterministic assembly of the
855 gut microbiome. *Appl Environ Microbiol* 2020; **86**: e00489-20.
856 76. Waite DW, Vanwonterghem I, Rinke C, Parks DH, Zhang Y, Takai K, et al.
857 Comparative genomic analysis of the class Epsilonproteobacteria and proposed
858 reclassification to Epsilonbacteraeota (phyl. nov.). *Front Microbiol* 2017; **8**.
859 77. Suzuki Y, Sasaki T, Suzuki M, Nogi Y, Miwa T, Takai K, et al. Novel
860 chemoautotrophic endosymbiosis between a member of the Epsilonproteobacteria and
861 the hydrothermal-vent gastropod *Alviniconcha aff. hessleri* (Gastropoda: Provannidae)
862 from the Indian Ocean. *Appl Environ Microbiol* 2005; **71**: 5440–5450.
863 78. Frias-Lopez J, Zerkle AL, Bonheyo GT, Fouke BW. Partitioning of bacterial
864 communities between seawater and healthy, black band diseased, and dead coral
865 surfaces. *Appl Environ Microbiol* 2002; **68**: 2214–2228.
866 79. Sunagawa S, DeSantis TZ, Piceno YM, Brodie EL, DeSalvo MK, Voolstra CR, et al.
867 Bacterial diversity and white plague disease-associated community changes in the
868 Caribbean coral *Montastraea faveolata*. *ISME J* 2009; **3**: 512–521.

bioRxiv preprint doi: https://doi.org/10.1101/2024.05.20.594925; this version posted May 20, 2024. The copyright holder for this preprint (which was not certified by peer review) is the author/funder, who has granted bioRxiv a license to display the preprint in perpetuity. It is made available under aCC-BY-NC-ND 4.0 International license.

869 80. Gignoux-Wolfsohn SA, Vollmer SV. Identification of candidate coral pathogens on
870 white band disease-infected staghorn coral. *PLOS ONE* 2015; **10**: e0134416.
871 81. Sun F, Yang H, Zhang X, Tan F, Shi Q. Response characteristics of bacterial
872 communities in multiple coral genera at the early stages of coral bleaching during El
873 Niño. *Ecol Indic* 2022; **144**: 109569.
874 82. Torres MJ, Simon J, Rowley G, Bedmar EJ, Richardson DJ, Gates AJ, et al. Nitrous
875 oxide metabolism in nitrate-reducing bacteria: Physiology and regulatory mechanisms.
876 In: Poole RK (ed). *Advances in Microbial Physiology*. 2016. Academic Press, pp 353–
877 432.
878 83. Jørgensen BB, Revsbech NP. Colorless sulfur bacteria, *Beggiatoa* spp. and *Thiovulum*
879 spp., in O_2 and H_2S microgradients. *Appl Environ Microbiol* 1983; **45**: 1261–1270.
880 84. Fenchel T. Motility and chemosensory behaviour of the sulphur bacterium *Thiovulum*
881 *majus*. *Microbiology* 1994; **140**: 3109–3116.
882 85. Thar R, Fenchel T. True chemotaxis in oxygen gradients of the sulfur-oxidizing
883 bacterium *Thiovulum majus*. *Appl Environ Microbiol* 2001; **67**: 3299–3303.
884 86. Weber M, de Beer D, Lott C, Polerecky L, Kohls K, Abed RMM, et al. Mechanisms of
885 damage to corals exposed to sedimentation. *Proc Natl Acad Sci U S A* 2012; **109**:
886 E1558-67.
887 87. Carlton RG, Richardson LL. Oxygen and sulfide dynamics in a horizontally migrating
888 cyanobacterial mat: Black band disease of corals. *FEMS Microbiol Ecol* 1995; **18**:
889 155–162.
890 88. Xia Y, Wang Y, Wang Y, Chin FYL, Zhang T. Cellular adhesiveness and cellulolytic
891 capacity in Anaerolineae revealed by omics-based genome interpretation. *Biotechnol*
892 *Biofuels* 2016; **9**: 111.

bioRxiv preprint doi: https://doi.org/10.1101/2024.05.20.594925; this version posted May 20, 2024. The copyright holder for this preprint (which was not certified by peer review) is the author/funder, who has granted bioRxiv a license to display the preprint in perpetuity. It is made available under aCC-BY-NC-ND 4.0 International license.

893 89. Campbell AG, Schwientek P, Vishnivetskaya T, Woyke T, Levy S, Beall CJ, et al.
894 Diversity and genomic insights into the uncultured Chloroflexi from the human
895 microbiota. *Environ Microbiol* 2014; **16**: 2635–2643.
896 90. Cleary DFR, Polónia ARM, Becking LE, de Voogd NJ, Purwanto, Gomes H, et al.
897 Compositional analysis of bacterial communities in seawater, sediment, and sponges in
898 the Misool coral reef system, Indonesia. *Mar Biodivers* 2018; **48**: 1889–1901.
899 91. Taniguchi A, Kuroyanagi Y, Aoki R, Eguchi M. Community structure and predicted
900 functions of actively growing bacteria responsive to released coral mucus in
901 surrounding seawater. *Microbes Environ* 2023; **38**: ME23024.
902 92. Taylor JA, Palladino G, Wemheuer B, Steinert G, Sipkema D, Williams TJ, et al.
903 Phylogeny resolved, metabolism revealed: functional radiation within a widespread
904 and divergent clade of sponge symbionts. *ISME J* 2021; **15**: 503–519.
905 93. Gonzalez-Zapata FL, Bongaerts P, Ramírez-Portilla C, Adu-Oppong B, Walljasper G,
906 Reyes A, et al. Holobiont diversity in a reef-building coral over its entire depth range
907 in the mesophotic zone. *Front Mar Sci* 2018; **5**.
908 94. Hernandez-Agreda A, Leggat W, Bongaerts P, Herrera C, Ainsworth TD. Rethinking
909 the coral microbiome: Simplicity exists within a diverse microbial biosphere. *mBio*
910 2018; **9**: 10.1128/mbio.00812-18.
911 95. Yancey PH, Heppenstall M, Ly S, Andrell RM, Gates RD, Carter VL, et al. Betaines
912 and dimethylsulfoniopropionate as major osmolytes in Cnidaria with endosymbiotic
913 dinoflagellates. *Physiol Biochem Zool* 2010; **83**: 167–173.
914 96. Neave MJ, Rachmawati R, Xun L, Michell CT, Bourne DG, Apprill A, et al.
915 Differential specificity between closely related corals and abundant *Endozoicomonas*
916 endosymbionts across global scales. *ISME J* 2017; **11**: 186–200.

bioRxiv preprint doi: https://doi.org/10.1101/2024.05.20.594925; this version posted May 20, 2024. The copyright holder for this preprint (which was not certified by peer review) is the author/funder, who has granted bioRxiv a license to display the preprint in perpetuity. It is made available under aCC-BY-NC-ND 4.0 International license.

97. Pogoreutz C, Ziegler M. Frenemies on the reef? Resolving the coral–*Endozoicomonas* association. *Trends Microbiol* 2024.

98. Deignan LK, Pwa KH, Loh AAR, Rice SA, McDougald D. The microbiomes of two Singaporean corals show site-specific differentiation and variability that correlates with the seasonal monsoons. *Coral Reefs* 2023; **42**: 677–691.

99. Jensen S, Duperron S, Birkeland N-K, Hovland M. Intracellular Oceanospirillales bacteria inhabit gills of Acesta bivalves. *FEMS Microbiol Ecol* 2010; **74**: 523–533.

100. Morris RL, Schmidt TM. Shallow breathing: bacterial life at low O2. *Nat Rev Microbiol* 2013; **11**: 205–212.

101. Guest JR, Green J, Irvine AS, Spiro S. The FNR Modulon and FNR-Regulated Gene Expression. In: Lin ECC, Lynch AS (eds). *Regulation of Gene Expression in Escherichia coli*. 1996. Springer US, Boston, MA, pp 317–342.

102. David LA, Weil A, Ryan ET, Calderwood SB, Harris JB, Chowdhury F, et al. Gut Microbial Succession Follows Acute Secretory Diarrhea in Humans. *mBio* 2015; **6**: 10.1128/mbio.00381-15.

103. Esposti MD, Romero EM. The functional microbiome of arthropods. *PLOS ONE* 2017; **12**: e0176573.

104. Wertz JT, Breznak JA. Physiological Ecology of Stenoxybacter acetivorans, an Obligate Microaerophile in Termite Guts. *Appl Environ Microbiol* 2007; **73**: 6829–6841.

105. Arai H. Regulation and function of versatile aerobic and anaerobic respiratory metabolism in *Pseudomonas aeruginosa*. *Front Microbiol* 2011; **2**: 103.

106. M'leod JW, Gordon J. Catalase production and sensitiveness to hydrogen peroxide amongst bacteria: With a scheme of classification based on these properties. *J Pathol Bacteriol* 1923; **26**: 326–331.

bioRxiv preprint doi: https://doi.org/10.1101/2024.05.20.594925; this version posted May 20, 2024. The copyright holder for this preprint (which was not certified by peer review) is the author/funder, who has granted bioRxiv a license to display the preprint in perpetuity. It is made available under aCC-BY-NC-ND 4.0 International license.

942 107. Brioukhanov AL, Netrusov AI. Catalase and Superoxide Dismutase: Distribution,
943 Properties, and Physiological Role in Cells of Strict Anaerobes. *Biochem Mosc* 2004;
944 **69**: 949–962.
945 108. Sun S, Jones RB, Fodor AA. Inference-based accuracy of metagenome prediction tools
946 varies across sample types and functional categories. *Microbiome* 2020; **8**: 1–9.
947 109. Toole DR, Zhao J, Martens-Habbena W, Strauss SL. Bacterial functional prediction
948 tools detect but underestimate metabolic diversity compared to shotgun metagenomics
949 in southwest Florida soils. *Appl Soil Ecol* 2021; **168**: 104129.
950
951

bioRxiv preprint doi: https://doi.org/10.1101/2024.05.20.594925; this version posted May 20, 2024. The copyright holder for this preprint (which was not certified by peer review) is the author/funder, who has granted bioRxiv a license to display the preprint in perpetuity. It is made available under aCC-BY-NC-ND 4.0 International license.

952 **Figure legends**

953 **Figure 1. The gastric cavity sampling set up.** Side (**a**) and top (**b**) view schematic illustration of the
954 microcapillary sampling set up. (**c**) Microneedle sampling set up. (**d**, **e**) Representative images of *L. hemprichii*
955 during sampling with a microneedle (**d**) and a microswab (**e**). Scale bars = 5 mm.

956

957 **Figure 2. The gastric cavity oxygen microenvironment of Great Barrier Reef corals.** Oxygen microsensor
958 profiles taken inside the gastric cavity of *D. favus* (**a**), *F. fungites* (**b**), *C. aspera* (**c**), and *L. hemprichii* (**d**)
959 collected from the Great Barrier Reef. Profiles taken under 650 µmol photons m^{-2} s^{-1} ("Light") or in darkness
960 ("Dark"). Arrows indicate 100% oxygen saturation under the measurement-specific temperature and salinity.
961 Each profile corresponds to one polyp (mean ± s.d., n=3 replicate profiles per polyp). (**e**) Average thickness of
962 GVC oxygen microniches calculated from the profiles in **a**-**d** (hyperoxic, normoxic, hypoxic and anoxic). Total
963 bar height represents GVC depth. (**f**) Oxygen concentration ranges for different regions of the digestive tract of
964 vertebrate and invertebrate animals (human, pig, dog, mouse, rabbit, caterpillar, grasshopper, beetle, termite,
965 isopod, sea urchin, sea cucumber, polychaete, *L. hemprichii* in darkness, *L. hemprichii* in the light). Data for
966 non-coral animals was calculated from the sources listed in Supplementary Table S3. The exact sections of
967 digestive tract for each organism are listed in Supplementary Table S3 (fore, mid and hind-gut are not the
968 technical nomenclature for all animals). For *L. hemprichii*, we considered three 2 mm thick sections of the GVC
969 (top, middle and bottom). The partial pressure of O_2 at sea level (21.22kPa) was considered as 100% saturation
970 for measurements performed in air, while 100% air saturation at the measurement temperature and salinity was
971 used for measurements performed in liquid media.

972

973 **Figure 3. Abundance and diversity of bacteria in the gastric cavity of GBR corals.** Bacterial cell counts (**a**)
974 and alpha diversity from 16S metabarcoding (**b**) for samples collected from the GVC and DBL of *D. favus*, *F.*
975 *pentagona*. *F. fungites*, *C. aspera*, and *L. hemprichii,* as well as the surrounding seawater. Spheres represent
976 individual data point, stars show $P<0.05$ in Tukey's HSD test following one-way ANOVA.

977

978 **Figure 4. Community composition of GVC microbiomes from GBR corals.** (**a**) Non-metric
979 multidimensional scaling (NMDS) based on Bray-Curtis dissimilarity of microbial communities found in the
980 gastric cavity (GVC) and diffusive boundary layer (DBL) of *D. favus*, *F. pentagona*, *F. fungites*, *G. fascicularis*,
981 *C. aspera* and *L. hemprichii*, as well as seawater (SW). (**b**) Relative abundance of taxa of interest, identified as

bioRxiv preprint doi: https://doi.org/10.1101/2024.05.20.594925; this version posted May 20, 2024. The copyright holder for this preprint (which was not certified by peer review) is the author/funder, who has granted bioRxiv a license to display the preprint in perpetuity. It is made available under aCC-BY-NC-ND 4.0 International license.

982 differentially abundant in coral samples by aldex Kruskal-Wallis test, in the different sample types. Spheres
983 indicate individual data points.
984
985 **Figure 5. The *L. hemprichii* microbiome on the GBR and in aquarium.** Alpha (**a**) and beta (**b**) diversity of
986 microbial communities isolated from the *L. hemprichii* gastric cavity (GVC) and diffusive boundary layer
987 (DBL) on the GBR immediately after collection (GBR1) and after 7 days in a flow-through aquarium (GBR2),
988 from the gastric cavity of captive *L. hemprichii* (UTS), as well as from seawater, holding tanks and flow
989 chamber. In (**a**), spheres represent individual data points.
990
991 **Figure 6. Core microbiome and predicted functional profiles in the *L. hemprichii* gastric cavity.** (**a**)
992 Cumulative abundance in different sample types of the 11 core ASVs shared by GBR and aquarium *L.*
993 *hemprichii*. Sample types: gastric cavity (GVC) and diffusive boundary layer (DBL) samples collected from *L.*
994 *hemprichii* (GBR *L. hem*) and other GBR corals, GVC samples from aquarium *L. hemprichii* (UTS *L. hem*), and
995 GBR seawater samples (GBR SW). (**b**) Cumulative abundance of taxa predicted to contain the genes coding for
996 high affinity terminal oxidases (cbb_3 and bd type), low affinity terminal oxidases (aa_3 and bo_3 types), ratio
997 between the two (y axis on log scale), and CRP/FNR family transcriptional regulator (*fnr*). Spheres represent
998 individual datapoints. In (**b**), stars represent adjusted $P<0.05$ in post-hoc Dunn's test following Kruskal-Wallis
999 test.

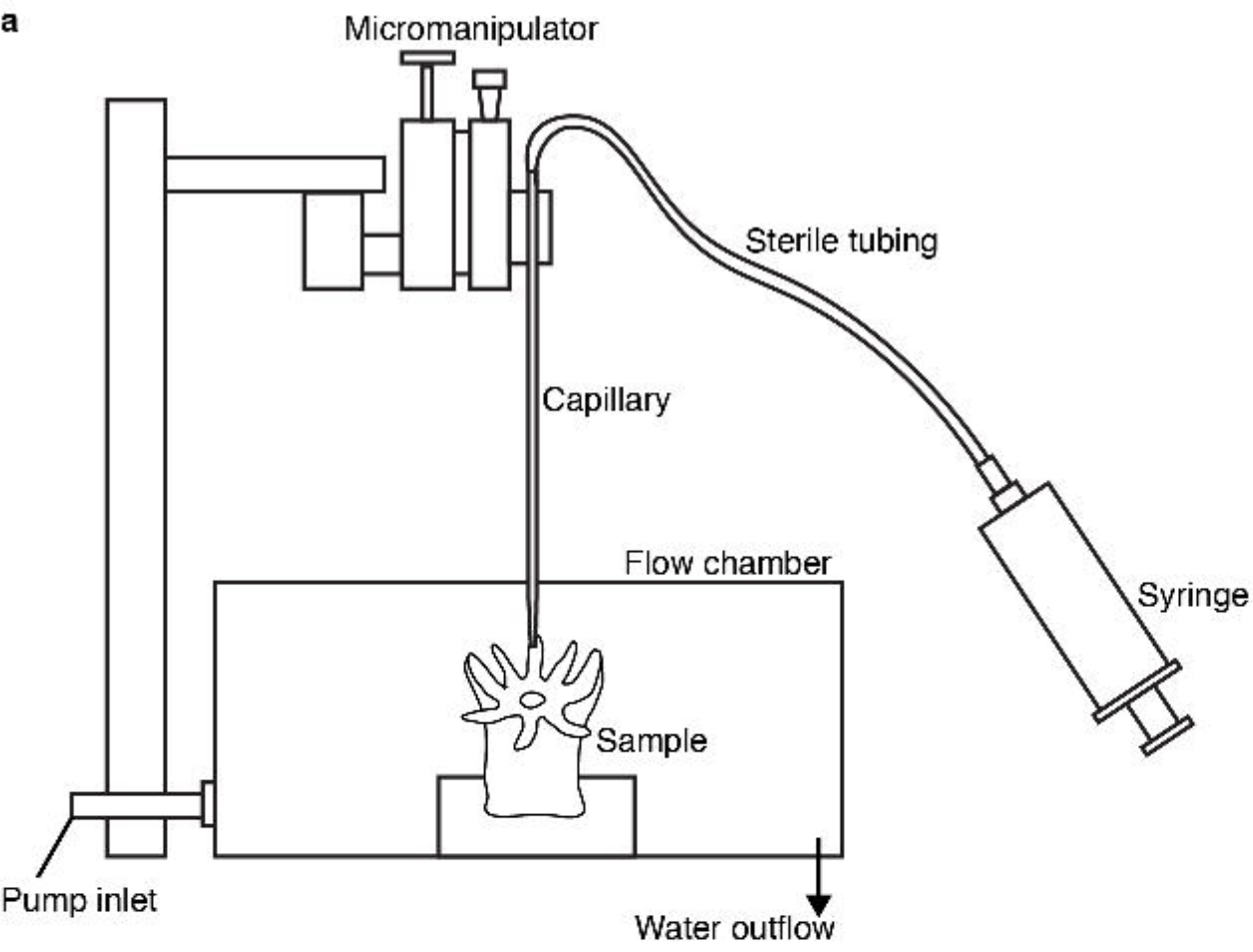
a
Micromanipulator
Sterile tubing
Capillary
Flow chamber
Syringe
Sample
Pump inlet
Water outflow

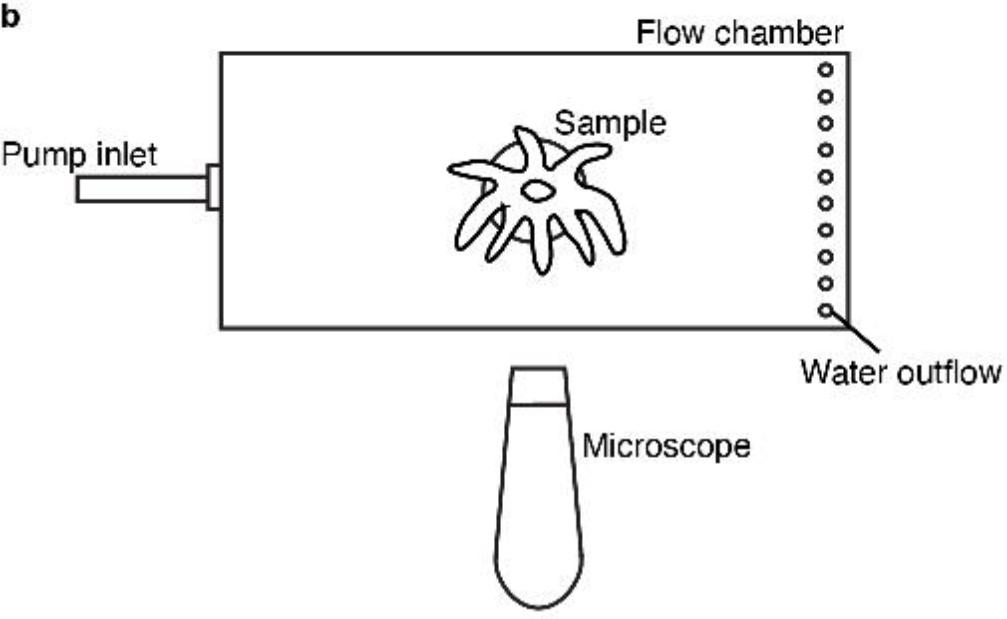
b
Flow chamber
Sample
Pump inlet
Water outflow
Microscope

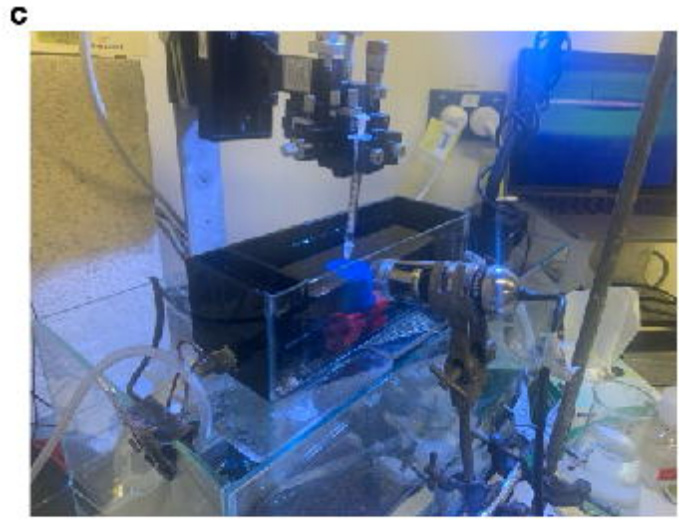
c

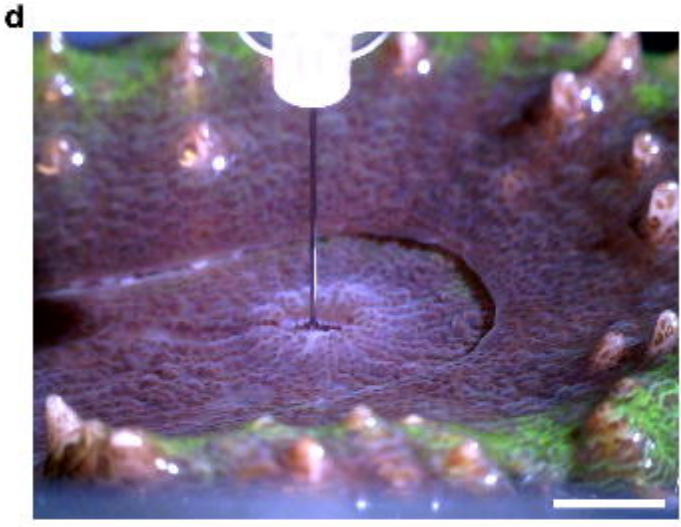
d

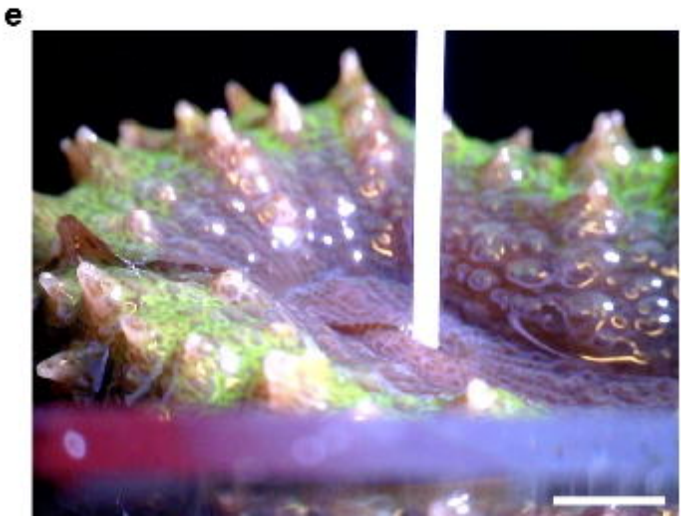
e

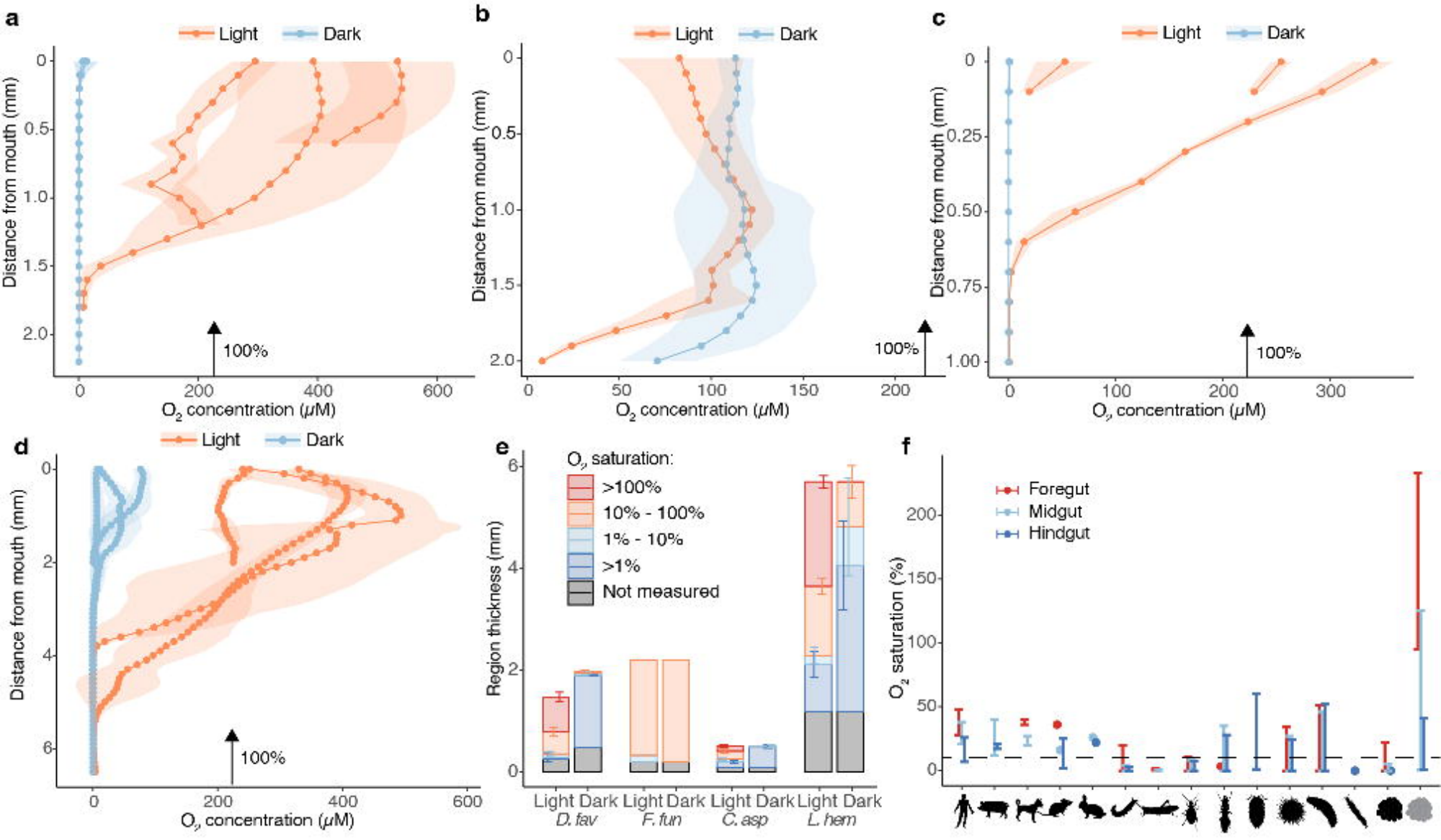
a
Light
Dark
Distance from mouth (mm)
0
0.5
1.0
1.5
2.0
100%
0
200
400
600
O2 concentration (μM)
b
Light
Dark
Distance from mouth (mm)
0
0.5
1.0
1.5
2.0
100%
0
50
100
150
200
O2 concentration (μM)
c
Light
Dark
Distance from mouth (mm)
0
0.25
0.50
0.75
1.00
100%
0
100
200
300
O2 concentration (μM)
d
Light
Dark
Distance from mouth (mm)
0
2
4
6
100%
0
200
400
600
O2 concentration (μM)
e
O2 saturation:
>100%
10% - 100%
1% - 10%
>1%
Not measured
Region thickness (mm)
0
2
4
6
Light Dark Light Dark Light Dark Light Dark
D. fav
F. fun
C. asp
L. hem
f
Foregut
Midgut
Hindgut
O2 saturation (%)
0
50
100
150
200

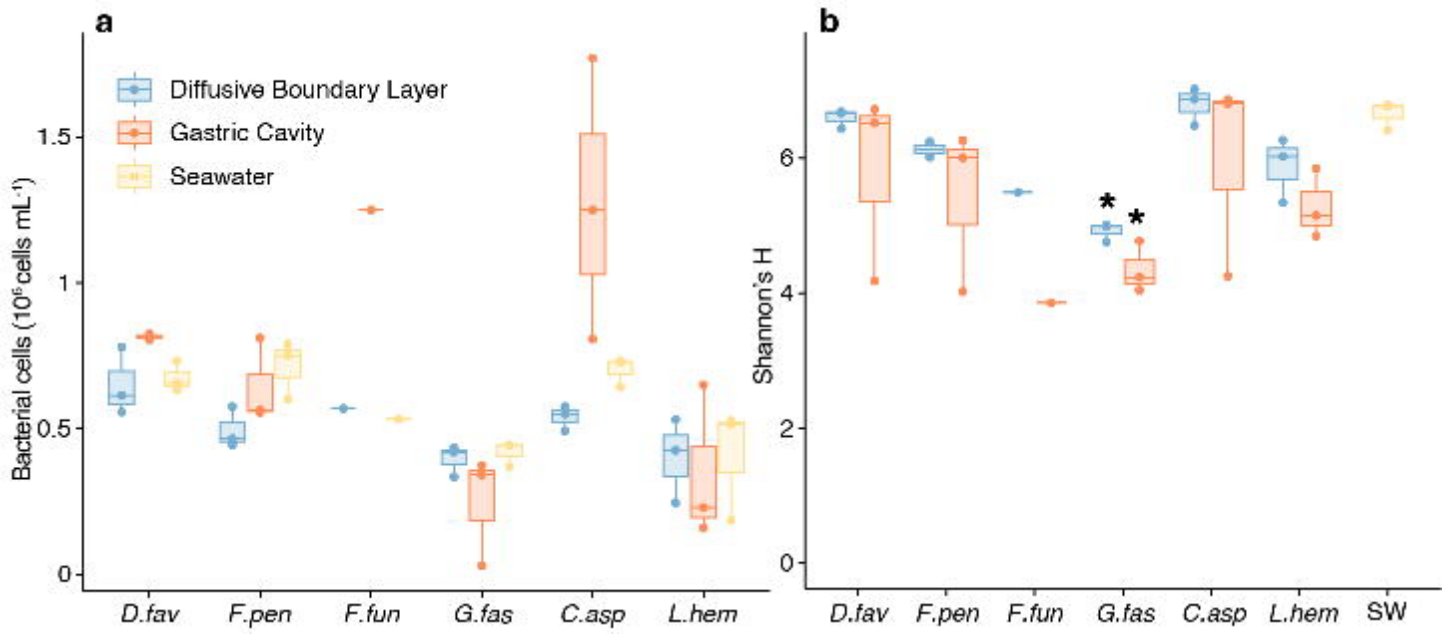
a
b
Diffusive Boundary Layer
Gastric Cavity
Seawater
Bacterial cells (10^6 cells mL^-1)
Shannon's H
1.5
1
0.5
0
6
4
2
0
*
*
D.fav
F.pen
F.fun
G.fas
C.asp
L.hem
SW

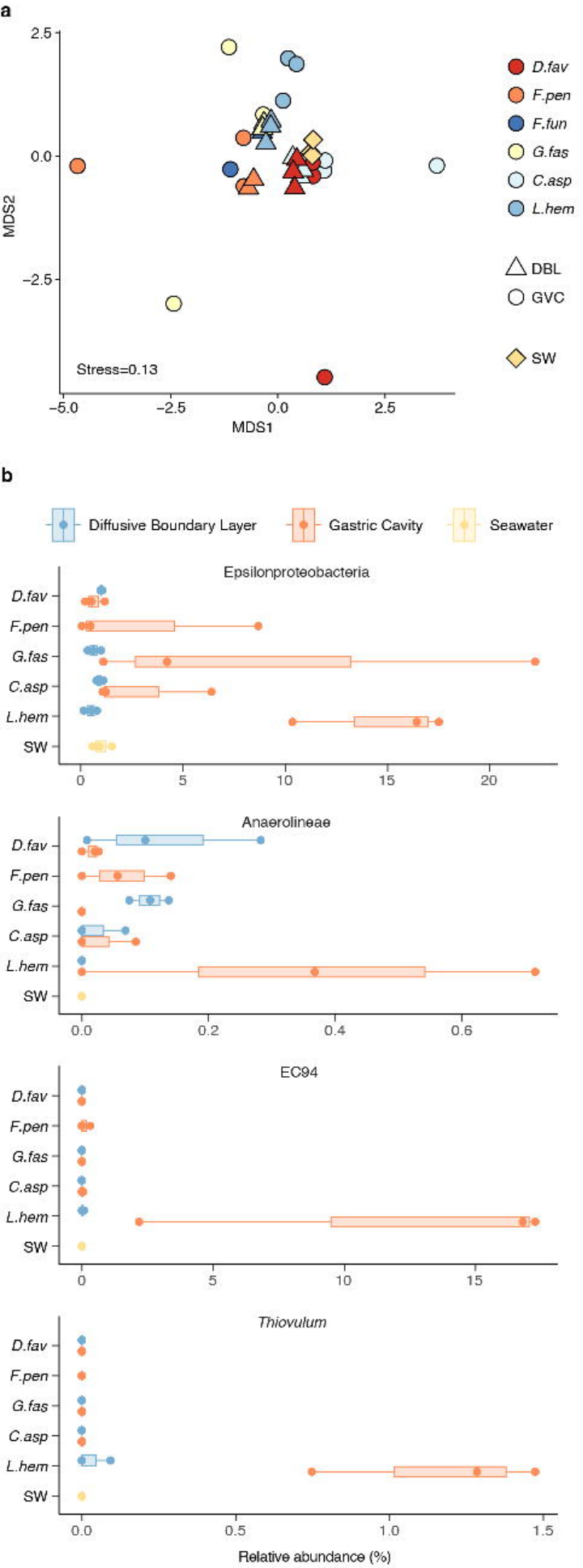
a
2.5
0.0
−2.5
MDS2
Stress=0.13
−5.0
−2.5
0.0
2.5
MDS1
D.fav
F.pen
F.fun
G.fas
C.asp
L.hem
DBL
GVC
SW
b
Diffusive Boundary Layer
Gastric Cavity
Seawater
Epsilonproteobacteria
D.fav
F.pen
G.fas
C.asp
L.hem
SW
0
5
10
15
20
Anaerolineae
0.0
0.2
0.4
0.6
EC94
Thiovulum
0.0
0.5
1.0
1.5
Relative abundance (%)

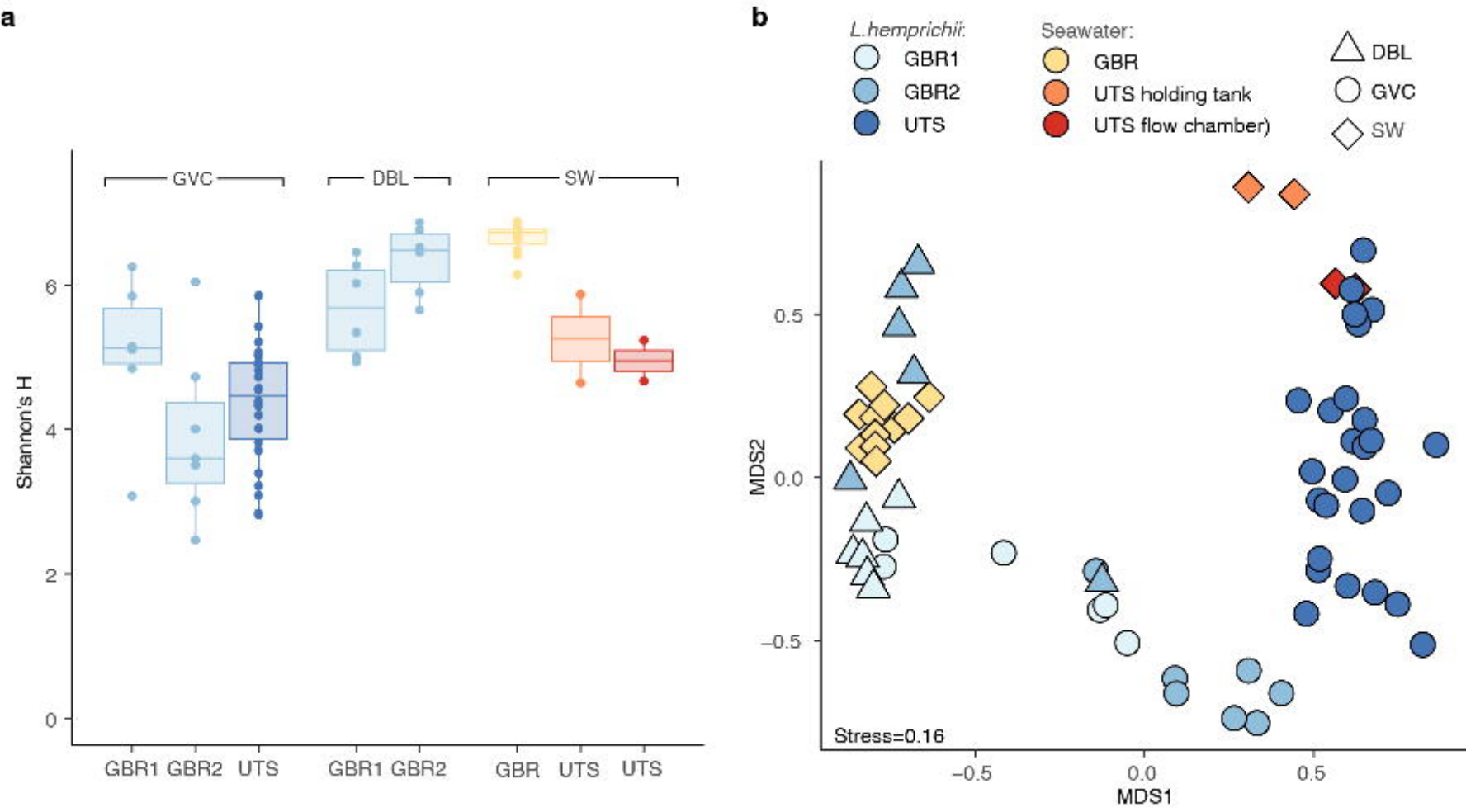
a
GVC
DBL
SW
Shannon's H
0
2
4
6
GBR1 GBR2 UTS
GBR1 GBR2
GBR UTS UTS
b
L.hemprichii:
GBR1
GBR2
UTS
Seawater:
GBR
UTS holding tank
UTS flow chamber)
DBL
GVC
SW
MDS2
0.5
0.0
−0.5
Stress=0.16
−0.5
0.0
0.5
MDS1

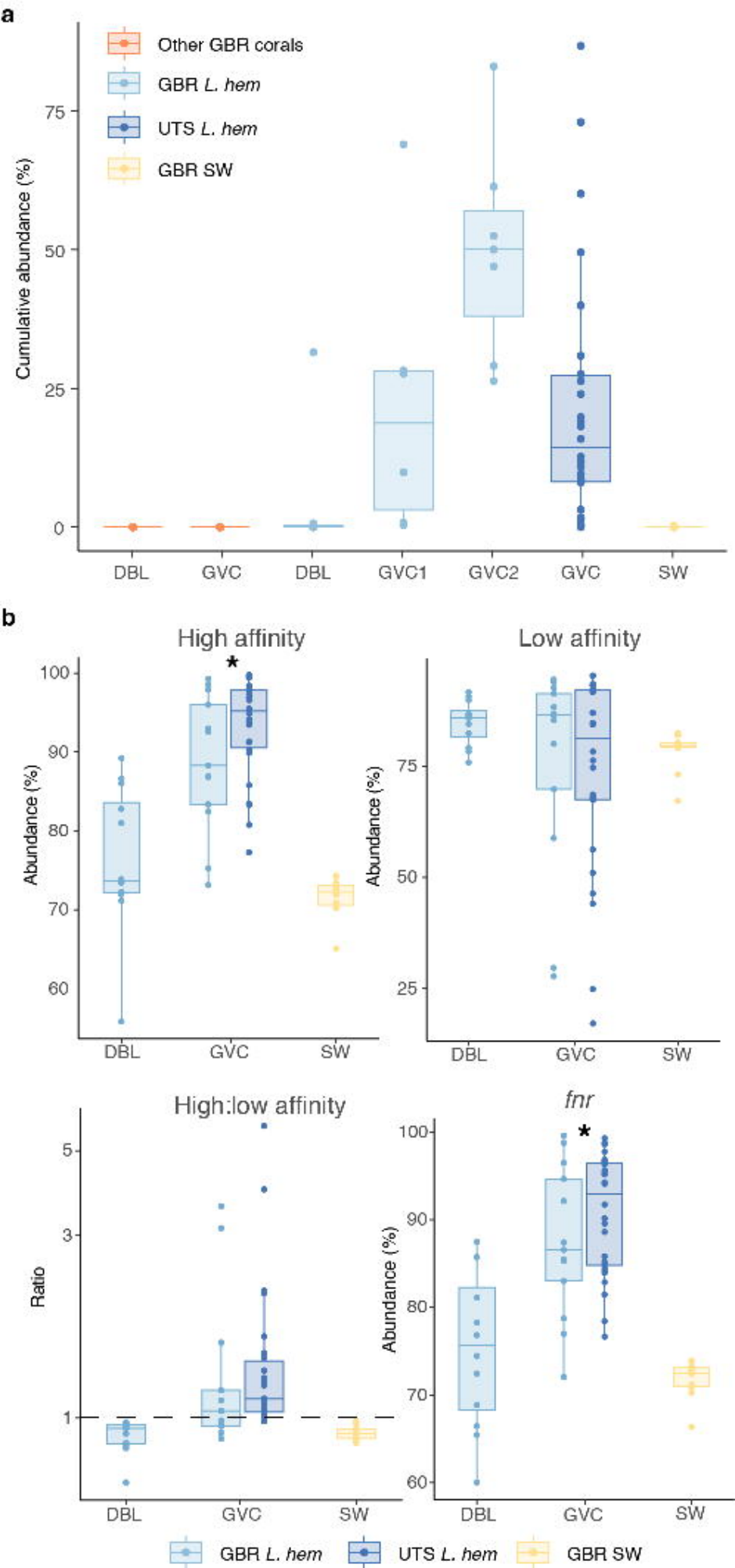
a
Other GBR corals
GBR L. hem
UTS L. hem
GBR SW
Cumulative abundance (%)
75
50
25
0
DBL
GVC
DBL
GVC1
GVC2
GVC
SW
b
High affinity
Low affinity
Abundance (%)
100
90
80
70
60
75
50
25
*
DBL
GVC
SW
High:low affinity
Ratio
5
3
1
fnr
GBR L. hem
UTS L. hem
GBR SW